



HAL
open science

Stable isotope patterns of mesopelagic communities over two shallow seamounts of the south-western Indian Ocean

Pavane Annasawmy, Yves Cherel, Evgeny V. Romanov, François Le Loc'h, Frédéric Ménard, Jean-François Ternon, Francis Marsac

► To cite this version:

Pavane Annasawmy, Yves Cherel, Evgeny V. Romanov, François Le Loc'h, Frédéric Ménard, et al.. Stable isotope patterns of mesopelagic communities over two shallow seamounts of the south-western Indian Ocean. *Deep Sea Research Part II: Topical Studies in Oceanography*, 2020, 176, pp.104804. 10.1016/j.dsr2.2020.104804 . hal-02871291

HAL Id: hal-02871291

<https://hal.science/hal-02871291>

Submitted on 22 Aug 2022

HAL is a multi-disciplinary open access archive for the deposit and dissemination of scientific research documents, whether they are published or not. The documents may come from teaching and research institutions in France or abroad, or from public or private research centers.

L'archive ouverte pluridisciplinaire **HAL**, est destinée au dépôt et à la diffusion de documents scientifiques de niveau recherche, publiés ou non, émanant des établissements d'enseignement et de recherche français ou étrangers, des laboratoires publics ou privés.



Distributed under a Creative Commons Attribution - NonCommercial 4.0 International License

Stable isotope patterns of mesopelagic communities over two shallow seamounts of the south-western Indian Ocean

Pavane Annasawmy^{1,2}, Yves Cherel³, Evgeny V. Romanov⁴, François Le Loc'h⁵, Frédéric Ménard⁶, Jean-François Ternon¹, Francis Marsac^{1,2}

¹ *MARBEC, IRD, Univ Montpellier, CNRS, Ifremer, Sète, France*

² *Department of Biological Sciences and Marine Research Institute/ICEMASA, University of Cape Town, Cape Town, South Africa*

³ *Centre d'Etudes Biologiques de Chizé (CEBC), UMR7372 du CNRS- La Rochelle Université, Villiers-en-Bois, France*

⁴ *Centre technique d'appui à la pêche réunionnaise (CAP RUN - CITEB), Île de la Réunion, France*

⁵ *IRD, Univ Brest, CNRS, Ifremer, LEMAR, IUEM, F-29280 Plouzane, France*

⁶ *Aix Marseille Univ, Université de Toulon, CNRS, IRD, MIO, UM110, Marseille, France*

* Corresponding author: angelee-pavane.annasawmy@ird.fr

ORCID Numbers:

Pavane Annasawmy: 0000-0001-8803-9687

Yves Cherel: 0000-0001-9469-9489

François Le Loc'h: 0000-0002-3372-6997

Frédéric Ménard: 0000-0003-1162-660X

Jean-François Ternon: 0000-0002-1396-8921

Francis Marsac: 0000-0002-3295-594X

Abstract

The stable carbon ($\delta^{13}\text{C}$) and nitrogen ($\delta^{15}\text{N}$) isotope values of soft tissues of micronekton (crustaceans, squid, mesopelagic fish) and zooplankton were measured from organisms collected on the RV *Antea* at two seamounts located in the south-western Indian Ocean: La Pérouse (summit depth ~60 m) and “MAD-Ridge” (thus named in this study; summit depth ~240 m). Surface particulate organic matter (POM-Surf) showed higher $\delta^{13}\text{C}$ at the more productive MAD-Ridge than at the oligotrophic La Pérouse seamount. Particulate organic matter and zooplankton were depleted in ^{15}N at La Pérouse pinnacle compared with MAD-Ridge. Gelatinous organisms and crustaceans occupied the lowest and intermediate trophic levels (TL ~2 and 3 respectively) at both seamounts. Mesopelagic fish and smaller-sized squid sampled at both seamounts occupied TL ~3 to 4, whereas the large nektonic squid, *Ommastrephes bartramii*, collected at MAD-Ridge only, exhibited a TL of ~5. The $\delta^{15}\text{N}$ values of common open-water mesopelagic taxa were strongly influenced by specimen size and feeding habits at both seamounts, with an increase in $\delta^{15}\text{N}$ values with increasing size. Carnivorous fish species sampled exclusively over the seamounts’ flanks and summits exhibited TL values of ~4, irrespective of their wide size ranges. The work could not demonstrate any differences in $\delta^{15}\text{N}$ values of mesopelagic fish between the seamounts and the surrounding oceanic areas. The study segregated clusters of mesopelagic organisms according to their $\delta^{13}\text{C}$ and $\delta^{15}\text{N}$ values, with variations in stable isotope values reflecting a complex range of processes possibly linked to productivity as well as biological and ecological traits of the species (size and feeding mode).

Keywords: micronekton, crustaceans, fish, $\delta^{13}\text{C}$, $\delta^{15}\text{N}$, trophic level

1 **1. Introduction**

2 Micronekton are a broad group of organisms mostly dwelling in the mesopelagic zone
3 (<1000 m). They consist of crustaceans (adult euphausiids, hyperiid amphipods, pelagic
4 decapods and mysids), cephalopods (small species and juvenile stages of large oceanic
5 species) and fish (mainly mesopelagic species and juveniles of pelagic fish) (Brodeur &
6 Yamamura, 2005; De Forest & Drazen, 2009; Ménard et al., 2014). They range in size from 2
7 to 20 cm and represent a substantial biomass in oceanic waters (Brodeur & Yamamura,
8 2005). Many species exhibit extensive diel vertical migrations (DVM), thus playing an
9 important role in the biological pump by transporting carbon and nutrients from the
10 epipelagic to the mesopelagic zone (Hidaka et al., 2001; Brodeur & Yamamura, 2005; Catul
11 et al., 2011; Bianchi et al., 2013). Micronekton also form a key trophic link between
12 zooplankton and top predators because they are preyed upon by several species of seabird,
13 tuna and billfish (Guinet et al., 1996; Bertrand et al., 2002; Brodeur & Yamamura, 2005;
14 Potier et al., 2007; Karakulak et al., 2009; Cherel et al., 2010; Danckwerts et al., 2014;
15 Jaquemet et al., 2014; Duffy et al., 2017; Watanuki & Thiebot, 2018). Various studies have
16 investigated the trophic interactions of micronekton to better understand their role in
17 foodwebs across numerous ocean basins (Fanelli et al., 2011b; Colaço et al., 2013; Fanelli et
18 al., 2013; Ménard et al., 2014; Valls et al., 2014a, b; Annasawmy et al., 2018). For instance,
19 mesopelagic organisms were shown to transfer energy between primary consumers and
20 deeper benthic and benthopelagic animals at Condor seamount in the Atlantic (Colaço et al.,
21 2013).

22 Tuna, billfish, pelagic armorheads, alfonosinos and orange roughy are common predators
23 fished extensively at seamounts in the Atlantic (Fonteneau, 1991; Morato et al., 2008;
24 Dubroca et al., 2013), Pacific (Rogers, 1994; Koslow, 1997; Holland et al., 1999; Musyl et
25 al., 2003; Paya et al., 2006; Morato et al., 2010) and Indian oceans (Romanov, 2003; Clark et

26 al., 2007; Marsac et al., 2014). Although, La Pérouse does not represent an outstanding
27 fishing spot, tuna (*Thunnus* spp.) and swordfish (*Xiphias gladius*) are present in the vicinity
28 of the seamount throughout the year (Marsac et al., 2020). Albacore (*Thunnus alalunga*),
29 bigeye (*T. obesus*), yellowfin (*T. albacares*) tuna and swordfish commonly occur along the
30 Madagascar Ridge and MAD-Ridge pinnacle (IOTC, www.iotc.org/data-and-statistics). The
31 Madagascar Ridge has also been targeted for orange roughy in 1999/2000 before the catch
32 dropped significantly in subsequent years (Ingole & Koslow, 2005; Lack et al., 2003). Due to
33 the increased pressure on marine organisms, characterizing the overall energy flow within
34 pelagic ecosystems (Young et al., 2015) contributes to making better informed fisheries and
35 ecosystem-based management decisions.

36 Two seamounts of the southwestern Indian Ocean (SWIO), La Pérouse and an unnamed
37 pinnacle, thereafter named “MAD-Ridge”, were studied in an effort to understand how
38 seamounts may affect diel vertical migrations and aggregations of micronekton (Annasawmy
39 et al., 2019, 2020). While micronekton acoustic densities were not significantly different
40 between the summit and immediate vicinity of the pinnacles, dense aggregations of scatterers,
41 referred to as seamount-associated species, were recorded over the summit of both seamounts
42 during day and night (Annasawmy et al., 2019). La Pérouse is situated in the Indian South
43 Subtropical Gyre (ISSG) province (Longhurst, 2007; Reygondeau et al., 2013) with low
44 mesoscale activities and primary productivity, whereas MAD-Ridge is located within an
45 “eddy corridor” to the south of Madagascar, in a region with high occurrence of cyclonic and
46 anticyclonic eddies and relatively high sea surface chlorophyll concentrations all year round
47 compared to La Pérouse (Halo et al., 2014; Annasawmy et al., 2019; Vianello et al., 2020).
48 The enhanced productivity on the Madagascar shelf and its offshore entrainment by
49 mesoscale eddy interactions (Quartly et al., 2006), were one possible reasons leading to
50 greater micronekton acoustic densities at MAD-Ridge relative to La Pérouse (Annasawmy et

51 al., 2020). Trapped, enclosed circulations known as Taylor columns may also develop over
52 seamounts and contribute to the retention of productivity (Genin & Boehlert, 1985; Dower et
53 al., 1992; Mouriño et al., 2001; Mohn & White, 2007). No Taylor columns were observed at
54 La Pérouse and MAD-Ridge seamounts, however, during the cruises most likely because of
55 the high current speeds observed over the summits and the seamount structure not being
56 favourable for the development and retention of such features (Annasawmy et al., 2020).

57 Foodwebs are shaped by a complex set of interactions controlled by the availability of
58 organic (C-based nutrients) and inorganic (such as nitrate, nitrite, phosphate and silicate)
59 nutrients, the efficiency of energy transfer to higher trophic levels and the control of species
60 biomass by predators (Pomeroy, 2001). Carbon ($\delta^{13}\text{C}$) and nitrogen ($\delta^{15}\text{N}$) stable isotope
61 analyses are a valuable tool for foodweb investigations in deep-sea ecosystems (Michener &
62 Kaufman, 2007) and are based on time-integrated assimilated food (Martínez del Rio et al.,
63 2009). Trophodynamic studies commonly employ $\delta^{13}\text{C}$ to investigate the source of organic
64 matter and $\delta^{15}\text{N}$ to determine trophic level and trophic interactions (Michener & Kaufman,
65 2007). The heavier isotopes (^{13}C and ^{15}N) are preferentially retained in tissues of consumers
66 relative to their prey, while lighter ^{12}C and ^{14}N isotopes are preferentially excreted (Fry,
67 2006). Overall, there is a small isotopic enrichment of 0.5-1‰ in the heavier ^{13}C isotope of
68 an organism's tissue relative to its diet (Fry, 2006). Differences in $\delta^{13}\text{C}$ values can thus
69 indicate different sources of primary production such as inshore vs offshore, or pelagic vs
70 benthic contributions to food intake (Hobson et al., 1994; Rubenstein & Hobson, 2004). In
71 contrast, $\delta^{15}\text{N}$ values increase stepwise by 2-4‰ in a consumer's tissue relative to its diet
72 (Vanderklift & Ponsard, 2003; Michener & Kaufman, 2007; Martínez Del Rio et al., 2009),
73 thus allowing the discrimination of trophic levels.

74 Identification of the trophic position of various biotic components of the pelagic ecosystem is
75 essential for our understanding of ecosystem functioning and trophic interactions. Food chain

76 length (i.e. number of TLs) is a descriptor of community structure and ecosystem functioning
77 (Post et al., 2000). Measuring the length of a food chain integrates the assimilation of energy
78 flow through all trophic pathways leading to top predators. The understanding of this is
79 essential from an ecosystem-based management perspective, and may provide important
80 insights on ecosystem responses to fisheries- pressure and/or climate-induced changes.
81 Knowledge of micronekton trophic interactions at seamount ecosystems of the SWIO are
82 scarce and fragmentary. In order to investigate the trophic pathways at La Pérouse and MAD-
83 Ridge, $\delta^{13}\text{C}$ and $\delta^{15}\text{N}$ values of POM, zooplankton and micronekton were measured and
84 trophic levels were estimated using additive isotopic models (as in Post, 2002, and Caut et al.,
85 2009). The main goals of this study were to investigate at La Pérouse and MAD-Ridge
86 seamounts, (1) the trophic interactions of sampled mesopelagic organisms, (2) the influence
87 of trophic groups, specimen size and time of sampling (MAD-Ridge only) on $\delta^{13}\text{C}$ and $\delta^{15}\text{N}$
88 values of micronekton, (3) the $\delta^{13}\text{C}$ and $\delta^{15}\text{N}$ values of omnivorous/carnivorous fish collected
89 over the flank relative to the vicinity of La Pérouse; and summit, flanks and vicinity of MAD-
90 Ridge compared with an off-seamount location in the southern Mozambique Channel.

91

92 **2. Material and methods**

93 2.1 Study sites

94 2.1.1 La Pérouse seamount

95 La Pérouse is located on the outskirts of the oligotrophic ISSG province (Longhurst, 1998,
96 2007; Reygondeau et al., 2013), 160 km northwest of Réunion Island at latitude $19^{\circ}43'S$ and
97 longitude $54^{\circ}10'E$ (Fig. 1a, b). The seamount summit reaches the euphotic zone, being ~60 m
98 below the sea surface. The summit is 10 km long with narrow and steep flanks and rises from

99 a depth of 5000 m from the ocean floor. The pinnacle was sampled on board the RV *Antea*
100 from 15 to 29 September 2016 (DOI: 10.17600/16004500).

101 2.1.2 MAD-Ridge seamount

102 This topographic feature, located ~240 km to the south of Madagascar, along the Madagascar
103 Ridge at latitude 27°29'S and longitude 46°16'E has been named "MAD-Ridge" in this study
104 (Fig. 1a, c). The seamount rises from a depth of 1600 m from the ocean floor to ~240 m
105 below the sea surface. The summit is 33 km long (north to south) and 22 km wide (east to
106 west). MAD-Ridge is surrounded by four smaller pinnacles, reaching depths of 600 m, 900
107 m, 800 m and 1200 m below the sea surface, between latitudes 27°S-28°S and longitudes
108 46°E-46°45'E. The MAD-Ridge pinnacle was sampled on board the RV *Antea* (DOI:
109 10.17600/16004800 and 10.17600/16004900) from 26 November to 14 December 2016.

110 2.2 Satellite observations

111 Sea surface chlorophyll data were downloaded from the MODIS dataset
112 (<http://oceancolor.gsfc.nasa.gov>) at a daily and 4.5 km resolution. Five-day averages were
113 calculated to obtain a proxy of phytoplankton abundance in the surface layer. To investigate
114 the annual variability in surface chlorophyll *a* concentrations, monthly mean concentrations
115 were averaged from January to December 2016 for the defined regions (La Perouse: 18.5-
116 20°S/53-33°E; MAD-Ridge: 27-28°S/44-48°E) (Fig. 2).

117 2.3 Sampling and sample processing

118 2.3.1 Particulate organic matter (POM)

119 During both cruises, water samples for stable isotope analyses of POM were collected using
120 Niskin bottles mounted on a Sea-Bird 911 + CTD rosette system at approximately 5 m depth
121 (referred to as POM-Surf) and at the depth of maximum fluorescence (referred to as POM-

122 Fmax) between ~60 and 125 m at La Pérouse and ~80 and 150 m at MAD-Ridge. Between 4
123 and 8 l (depending on the load of each sample) of seawater were filtered on precombusted 25
124 or 47 mm glassfibre of 0.7 µm pore size. The filters were oven-dried at 50°C for 24 h and
125 saved at room temperature in aluminium foil until further analyses.

126 2.3.2 Zooplankton sampling

127 Zooplankton samples were collected during daylight only with a Bongo net (300 µm mesh to
128 a maximum depth of 500 m and 200 µm mesh to a maximum depth of ~200 m) towed
129 obliquely at La Pérouse (10 stations). At MAD-Ridge, zooplankton samples were also
130 collected during daylight with a Bongo net (300 µm mesh to a maximum depth of 500 m
131 towed obliquely and 63 µm mesh to the depth of the maximum fluorescence towed vertically)
132 at 19 stations. The nets were fitted with a flowmeter and were towed at a vessel speed of 1.5-
133 2 knots for 15-20 min (0.28 m² mouth area). Zooplankton samples from the 200 and 300 µm
134 meshes at La Pérouse and, from the 63 and 300 µm meshes at MAD-Ridge were combined at
135 each station. The combined samples at each station were sieved on a stack of seven sieves of
136 decreasing mesh size and divided into six fractions: >4000 µm, 4000-2000 µm, 2000-1000
137 µm, 1000-500 µm, 500-250 µm, 250-125 µm during La Pérouse and MAD-Ridge and a 7th
138 fraction (125-63 µm) during MAD-Ridge only. Each fraction was oven-dried at 50°C for 24 h
139 and frozen on board at -20°C before being analysed for stable isotope analyses (section 2.4).
140 Zooplankton abundances, biomasses and taxa composition at the seamounts and off-
141 seamount locations are investigated in Noyon et al. (2020).

142 2.3.3 Trawl sampling

143 During both cruises, a 40-m long International Young Gadoid Pelagic Trawl (IYGPT) net
144 (codend with 0.5 cm knotless nylon delta mesh; front tapering end with 8 cm mesh; ~96 m²
145 mouth opening) was towed at a vessel speed of 2-3 knots for 60 mins during La Pérouse and

146 for 30 min during MAD-Ridge to sample mesopelagic organisms. Trawls were carried out in
147 the shallow (0-200 m), intermediate (200-400 m) and deep (below 400 m) layers during both
148 cruises (Supplementary Material, Table 1). Trawl stations at La Pérouse and MAD-Ridge
149 (Fig. 1b, c) were further classified into the categories summit, flank and vicinity- according to
150 whether they occurred on the summit plateau of the seamounts, along the flanks (seafloor
151 depth of 300-1300 m) or in the immediate vicinity (depth >1300 m) (Supplementary
152 Material, Table 1). Four other mesopelagic trawls (#18-21) were conducted in the southern
153 Mozambique Channel (depth >4000 m) during the MAD-Ridge cruise as reference stations
154 for non-seamount locations within the EAFR province (Fig. 1a).

155 All organisms collected with the trawl were sorted on board, divided into four broad
156 categories (gelatinous, crustaceans, cephalopods and fish), counted and identified to the
157 lowest possible taxon. Individuals from these four broad categories were randomly selected
158 according to their occurrence and abundance and measured (total length for selected
159 gelatinous organisms, abdomen and carapace length for selected crustaceans, dorsal mantle
160 length for cephalopods and standard length for fish). Approximately 2 to 5 mg of soft tissues
161 of these selected individuals (muscle tissue for leptocephali, muscle abdomen for crustaceans,
162 mantles for squid, dorsal muscle for fish) and whole salps and pyrosomes, were sampled on
163 board in 2 ml Eppendorf tubes and stored at -20°C, before being processed in the laboratory
164 to determine $\delta^{13}\text{C}$ and $\delta^{15}\text{N}$ values (section 2.4). A list of selected gelatinous and micronekton
165 taxa used in stable isotope analyses is given in Supplementary Material, Table 2.

166 2.4 Stable isotope analysis

167 Micronekton and zooplankton samples were freeze-dried using Christ Alpha 1-4 LSC freeze-
168 dryers for 48 h and ground to a fine homogeneous powder using an automatic ball mill
169 RETSCH MM200. As variations in lipid composition may influence $\delta^{13}\text{C}$ and $\delta^{15}\text{N}$ values

170 (Bodin et al., 2009; Ryan et al., 2012), lipids were removed from zooplankton and
171 micronekton samples with dichloromethane on an accelerated solvent extraction system
172 (ASE®, Dionex; Bodin et al., 2009). Prior to $\delta^{13}\text{C}$ analyses, POM filters and zooplankton
173 samples were reacted with 1 N HCl to remove carbonates (Cresson et al., 2012). Untreated
174 subsamples of POM and zooplankton were used to measure $\delta^{15}\text{N}$ because acid treatment may
175 lead to the loss of nitrogenous compounds (Kolasinski et al., 2008). POM filters were cut,
176 folded and put into tin capsules. Approximately 400-600 μg of each zooplankton and
177 micronekton sample were weighed and placed in tin capsules. These samples were run
178 through continuous flow on a Thermo Scientific Flash EA 2000 elemental analyser coupled
179 to a Delta V Plus mass spectrometer at the Pôle de Spectrométrie Océan (Plouzané, France).
180 The samples were combusted in the elemental analyser to separate CO_2 and N_2 . A reference
181 gas set was used to determine isotopic ratios by comparison. The isotopic ratios are expressed
182 in the conventional δ notations as parts per thousand (‰) deviations from the international
183 standards:

$$184 \quad \delta^{13}\text{C} \text{ or } \delta^{15}\text{N} (\text{‰}) = [(R_{\text{sample}}/R_{\text{standard}}) - 1] \times 1000$$

185 where R is the ratio of $^{13}\text{C}/^{12}\text{C}$ or $^{15}\text{N}/^{14}\text{N}$.

186 2.5 Data analyses

187 2.5.1 Overall $\delta^{13}\text{C}$ and $\delta^{15}\text{N}$ signatures

188 Shapiro-Wilk and Bartlett tests were computed to test for assumptions of normality and
189 homogeneity of variances. Links between $\delta^{13}\text{C}$ and $\delta^{15}\text{N}$ values and the foodweb components
190 (POM-Surf, POM-Fmax, zooplankton, gelatinous organisms, crustaceans, squid and fish),
191 were investigated using Kruskal-Wallis (KW) tests and pairwise comparisons in R (version
192 3.3.1) because the data did not follow normal distributions. Kruskal-Wallis tests and pairwise
193 comparisons were also computed to investigate whether there was a significant difference in

194 $\delta^{13}\text{C}$ and $\delta^{15}\text{N}$ values for each foodweb component between La Pérouse and MAD-Ridge. To
195 assess the association between $\delta^{13}\text{C}$ and $\delta^{15}\text{N}$ values, Spearman rank correlation coefficients
196 were calculated with all foodweb components at each seamount. Wilcoxon rank sum tests
197 investigated the effect of time (day or night) on $\delta^{13}\text{C}$ and $\delta^{15}\text{N}$ values of gelatinous plankton
198 and micronekton at MAD-Ridge only (because a single daylight trawl was conducted at La
199 Pérouse and too few species were caught). To test for the effect of trawl position with respect
200 to the seamounts on $\delta^{13}\text{C}$ and $\delta^{15}\text{N}$ values of omnivorous/carnivorous fish, Wilcoxon Rank
201 sum tests and KW tests were performed on the La Pérouse and MAD-Ridge datasets,
202 respectively.

203 2.5.2 Layman community-wide metrics

204 The Layman community-wide metrics SEA_c and the $\delta^{13}\text{C}$ and $\delta^{15}\text{N}$ ranges (Layman et al.,
205 2007) were calculated using the SIBER package (version 2.1.4, Jackson et al., 2011). The
206 SEA_c (sample-size-corrected standard ellipse area) describes the overall extent of the isotopic
207 niches. The SEA_c is robust for sample sizes >10 (Daly et al., 2013), which is the case for all
208 the broad categories within this study. The SEA_c of each foodweb component was described
209 in terms of the space occupied by the group on a $\delta^{15}\text{N}$ - $\delta^{13}\text{C}$ plot based on all the individuals
210 sampled within the group. The $\delta^{13}\text{C}$ and $\delta^{15}\text{N}$ ranges were used to describe and compare the
211 overall extents of the foodwebs at the La Pérouse and MAD-Ridge sites. Increased $\delta^{13}\text{C}$ range
212 would be expected in foodwebs with multiple basal sources with varying $\delta^{13}\text{C}$ values
213 suggesting niche diversification at the base of the foodweb, whereas the $\delta^{15}\text{N}$ range describes
214 the sampled food chain lengths (Portail et al., 2016).

215 2.5.3 Trophic level estimations

216 Different models have been applied across several studies to estimate the trophic level of
217 organisms: additive model with a fixed enrichment factor, additive enrichment model with a

218 variable isotopic enrichment or scaled model with decreasing isotopic enrichment factors
219 (Minagawa & Wada, 1984; Post, 2002; Caut et al., 2009; Hussey et al., 2014). Ménard et al.
220 (2014) and Annasawmy et al. (2018) used a fixed enrichment factor of 3.2‰ to estimate
221 trophic levels of foodweb components POM, zooplankton, gelatinous plankton and
222 micronekton collected in the SWIO. In this study, two alternative trophic enrichment
223 assumptions were compared to estimate the trophic level of all the measured individuals
224 within the groups (zooplankton, gelatinous organisms, crustaceans, squid and fish) at La
225 Pérouse and MAD-Ridge.

226 The TPA model (additive model with constant isotopic enrichment) was proposed by
227 Minagawa & Wada (1984) and Post (2002) with the reference level set at a trophic level of 2
228 for the primary consumer and a fixed and additive enrichment factor of 3.2‰:

$$229 \text{ Trophic level, TPA} = 2.0 + \frac{\delta^{15}\text{N}_i - \delta^{15}\text{N}_{\text{primary consumer}}}{3.2} \quad \text{Eq. 1}$$

230 where, $\delta^{15}\text{N}_i$ the nitrogen isotopic composition of any given micronekton taxon i , $\delta^{15}\text{N}_{\text{primary}}$
231 consumer the $\delta^{15}\text{N}$ reference baseline value at trophic level 2, and 3.2‰ is an estimate of the
232 trophic enrichment factor between consumers and their primary prey (Michener & Kaufman,
233 2007; Vanderklift & Ponsard, 2003). The $\delta^{15}\text{N}$ values of POM, primary consumers and
234 zooplankton have been used in trophic level calculations as isotopic baseline (e.g. Lorrain et
235 al., 2015). Primary consumers are generally used as baseline to reduce errors in estimations
236 (Martínez Del Rio et al., 2009). Salps are known filter feeders which have been used as
237 baseline in previous studies in the region (Ménard et al., 2014). At La Pérouse, the mean $\delta^{15}\text{N}$
238 values of six pyrosomes and one salp specimen was estimated at $5.31 \pm 0.31\text{‰}$ and was used
239 as $\delta^{15}\text{N}_{\text{primary consumer}}$ to estimate the trophic position of all upper trophic level individuals that
240 were collected. At MAD-Ridge, the mean $\delta^{15}\text{N}$ values of six salps was $4.22 \pm 1.01\text{‰}$ and was
241 used as $\delta^{15}\text{N}_{\text{primary consumer}}$ to estimate the trophic position of all individuals sampled.

242 The second model, TPC, is an additive trophic enrichment model with variable isotopic
243 enrichment, estimated from a meta-analysis study on fish muscle (Caut et al. 2009):

244 $TEF = -0.281 \delta^{15}N_{\text{primary consumer}} + 5.879$, where TEF is the trophic enrichment factor

245 $TPC = 2.0 + [(\delta^{15}N_i - \delta^{15}N_{\text{primary consumer}})/TEF]$ Eq. 2

246 2.5.4 Micronekton habitat ranges and feeding mode

247 Information on habitat ranges of selected micronekton individuals was obtained from the
248 literature (Clarke & Lu, 1975; Percy et al., 1977; Smith & Heemstra, 1986; van der Spoel &
249 Bleeker, 1991; Brodeur & Yamamura, 2005; Davison et al., 2015; Romero-Romero et al.,
250 2019). Organisms were classified as being epipelagic (<200 m), mesopelagic (from 200 to
251 1000 m), bathypelagic (below 1000 m to ~100 m from the seafloor) and benthopelagic (living
252 near the bottom) according to definitions of the vertical zonation of the pelagic ocean from
253 Del Giorgio & Duarte (2002) and Sutton (2013). The feeding modes of gelatinous plankton
254 and selected micronekton were obtained from the literature and are summarised in
255 Supplementary Material, Table 2. Organisms were classified into the four trophic groups
256 filter-feeders (salps and pyrosomes), detritivores (leptocephali), omnivores (mainly
257 crustaceans and the fish species *Ceratoscopelus warmingii*) and carnivores (most
258 mesopelagic fish and squid). Crustaceans were classified as omnivores because they prey on
259 zooplankton, such as euphausiids and copepods and are also known for occasional herbivory
260 (Hopkins et al., 1994; Birkley & Gulliksen, 2003; Mauchline, 1959; Foxton & Roe, 1974).
261 Most mesopelagic fish were classified as carnivores because they were reported to be
262 zooplankton feeders, preying on copepods, amphipods, euphausiids and ostracods
263 (Dalpadado & Gjørseter, 1988; Pakhomov et al., 1996; Tanaka et al., 2007; Hudson et al.,
264 2014; Bernal et al., 2015; Carmo et al., 2015; Young et al., 2015), with no herbivorous
265 feeding strategy except *C. warmingii*, which has developed an adaptive response to

266 competition in low-productive environments (Robison, 1984). For species with unknown
267 diets, the feeding mode was determined based on the feeding habit identified from species
268 within the same genus.

269 In order to give an overview of the foodwebs at the La Pérouse and MAD-Ridge seamounts,
270 hierarchical cluster analyses (average grouping methods) were carried out on resemblance
271 matrices (calculated using Euclidean distances) of normalised $\delta^{13}\text{C}$ and $\delta^{15}\text{N}$ values per
272 gelatinous plankton and micronekton species at each seamount and for all sampled stations in
273 PRIMER v6 software according to Clarke & Warwick (2001). Further cluster analyses were
274 performed on log-transformed $\delta^{13}\text{C}$ values and normalised $\delta^{13}\text{C}$ and $\delta^{15}\text{N}$ values of
275 micronekton (excluding the outliers salps, pyrosomes, *Funchalia* sp. and leptocephali) for
276 each seamount.

277 2.5.5 Effect of size on $\delta^{15}\text{N}$ values of micronekton

278 The size distributions of all gelatinous and micronekton organisms captured during the La
279 Pérouse and MAD-Ridge cruises were heavily right-skewed with most organisms being <100
280 mm in length due to net catchability and selectivity. To test for the effect of size on $\delta^{15}\text{N}$
281 values, gelatinous and micronekton organisms <100 mm were considered and linear
282 regressions were computed. Linear models were developed to investigate the effect of body
283 lengths on $\delta^{13}\text{C}$ and $\delta^{15}\text{N}$ values of gelatinous and micronekton individuals and to investigate
284 the difference in $\delta^{15}\text{N}$ values with respect to size between La Pérouse and MAD-Ridge.
285 Additionally, eight micronekton specimens were selected according to their common
286 occurrence at both seamounts, relatively large sample sizes and wide body length ranges, and
287 their $\delta^{15}\text{N}$ values were compared between the two seamounts. Information on the migration
288 patterns of these eight taxa was obtained from the literature (Utrecht et al., 1987; Butler et al.,
289 2001; Feunteun et al., 2015; Romero-Romero et al., 2019). Linear regressions were fitted to

290 $\delta^{15}\text{N}$ values of these eight taxa according to their body lengths and the seamount factor
291 (whether $\delta^{15}\text{N}$ values were significantly different between La Pérouse and MAD-Ridge). To
292 investigate if the seamount has an effect on the size and related diet of fish, $\delta^{15}\text{N}$ values of
293 selected omnivorous/ carnivorous fish species collected on the summits, flanks, vicinity of
294 the seamounts and the southern Mozambique Channel, were examined using linear models.

295 **3. Results**

296 3.1 Prevailing environmental conditions at La Pérouse and MAD-Ridge seamounts

297 Sea surface chlorophyll concentrations followed the same seasonal pattern in both regions of
298 La Pérouse and MAD-Ridge seamounts, although concentrations were twice as high at
299 MAD-Ridge (0.10-0.22 mg m^{-3}) than at La Pérouse (0.04-0.13 mg m^{-3}) all year round (Fig.
300 2). A peak in productivity was observed in July in both the ISSG and EAFR provinces
301 because of intense mixing caused by austral trade winds. Both La Pérouse and MAD-Ridge
302 cruises took place during a declining phase of oceanic productivity in the region.

303 3.2 General foodweb structure

304 The description of the foodweb structure included POM collected at the surface (POM-Surf)
305 and at the depth of maximum fluorescence (POM-Fmax), zooplankton at both seamounts,
306 two taxonomic groups of gelatinous organisms (salps and pyrosomes), and 42 and 49
307 taxonomic groups of micronekton, representing 145 and 180 individuals at La Pérouse and
308 MAD-Ridge respectively. At both La Pérouse and MAD-Ridge, the foodweb components
309 were segregated in their $\delta^{13}\text{C}$ (La Pérouse: KW, $H=170.5$, $p < 0.05$; MAD-Ridge: KW,
310 $H=268.1$, $p < 0.05$) and $\delta^{15}\text{N}$ values (La Pérouse: KW, $H=153.1$, $p < 0.05$; MAD-Ridge: KW,
311 $H=127.4$, $p < 0.05$) (Fig. 3). POM-Surf and POM-Fmax did not differ significantly in their
312 $\delta^{13}\text{C}$ and $\delta^{15}\text{N}$ values at both seamounts ($p > 0.05$). At La Pérouse, gelatinous organisms
313 exhibited higher $\delta^{13}\text{C}$ values compared with POM-Surf and POM-Fmax ($p < 0.05$), and they

314 exhibited lower $\delta^{13}\text{C}$ and $\delta^{15}\text{N}$ values than crustaceans, fish and squid at both seamounts ($p <$
315 0.05). Crustaceans, fish and squid did not differ significantly in their $\delta^{15}\text{N}$ values ($p > 0.05$),
316 but they differed in their $\delta^{13}\text{C}$ values at La Pérouse ($p < 0.05$). Crustaceans did not differ
317 significantly from squid in their $\delta^{13}\text{C}$ values ($p > 0.05$), whereas all other categories differed
318 in their $\delta^{13}\text{C}$ values at MAD-Ridge ($p < 0.05$). Squid did not differ significantly from
319 crustaceans and fish in their $\delta^{15}\text{N}$ values ($p > 0.05$), but ^{15}N was more depleted in crustaceans
320 relative to fish at MAD-Ridge ($p < 0.05$). At La Pérouse (all depths combined), POM,
321 zooplankton and micronekton covered a large $\delta^{13}\text{C}$ range of $\sim 11\text{‰}$ (-17.2 to -28.0‰), with
322 POM-Fmax and the unidentified caridean crustacean representing the lowest and highest
323 values, respectively. The $\delta^{15}\text{N}$ values of all micronekton individuals ranged from 2.5‰ (fish:
324 leptocephali) to 13.3‰ (fish: *Coccorella atrata*). At MAD-Ridge (all depths combined),
325 POM, zooplankton and micronekton also covered a large $\delta^{13}\text{C}$ range of $\sim 10\text{‰}$ (-17.1 to $-$
326 27.2‰), with POM-Surf and the fish species *Chauliodus sloani* representing the lowest and
327 highest values, respectively. The $\delta^{15}\text{N}$ values of sampled micronekton individuals ranged
328 from 2.3‰ (fish: leptocephali) to 13.5‰ (fish: *Argyropelecus aculeatus*).

329 Standard ellipse corrected areas (SEAc) refer to the trophic niche widths of the broad
330 categories at La Pérouse and MAD-Ridge. At La Pérouse, POM-Surf and POM-Fmax
331 showed overlapping standard ellipses with the largest SEAc (3.2 and 3.8‰^2 , respectively)
332 among all components of the foodweb (Fig. 3). Gelatinous organisms showed the smallest
333 SEAc of 0.92‰^2 . Crustaceans, squid and fish had overlapping standard ellipses with SEAc
334 values of 2.3 , 1.2 and 2.9‰^2 , respectively (Fig. 3). At MAD-Ridge, POM-Surf and POM-
335 Fmax also exhibited overlapping standard ellipses ($\text{SEAc} = 4.8$ and 2.0‰^2 , respectively), but
336 with greater variability in POM-Surf $\delta^{15}\text{N}$ values. Crustaceans, squid and fish had
337 overlapping standard ellipses with SEAc of 3.0 , 3.6 and 3.2‰^2 , respectively.

338 The $\delta^{13}\text{C}$ and $\delta^{15}\text{N}$ values of the foodweb components POM-Surf, POM-Fmax, zooplankton,
339 gelatinous organisms, crustaceans, squid and fish were significantly different between La
340 Pérouse and MAD-Ridge ($\delta^{13}\text{C}$: KW, $H=474.4$, $df=13$, $p < 0.05$; $\delta^{15}\text{N}$: KW, $H=311.3$, $df=13$,
341 $p < 0.05$, Fig. 4). Pairwise comparisons showed $\delta^{13}\text{C}$ values of POM-Surf, zooplankton and
342 fish to differ significantly between La Pérouse and MAD-Ridge ($p < 0.05$ each). The median
343 $\delta^{13}\text{C}$ and $\delta^{15}\text{N}$ values of lower trophic level foodweb components: POM-Surf, POM-Fmax
344 and zooplankton were greater at MAD-Ridge ($\delta^{13}\text{C}$: -23.1, -24.1, -20.9‰; $\delta^{15}\text{N}$: 6.3, 6.1 and
345 8.9‰, respectively) than at La Pérouse ($\delta^{13}\text{C}$: -23.7, -24.1, -22.1‰; $\delta^{15}\text{N}$: 5.5, 4.9 and 7.5‰,
346 respectively) (Fig. 4). Gelatinous organisms, crustaceans and fish displayed higher median
347 $\delta^{13}\text{C}$ values at La Pérouse (-21.5, -18.4 and -18.7‰, respectively) than at MAD-Ridge (-22.4,
348 -18.6 and -19.1‰, respectively) (Fig. 4). Gelatinous organisms, crustaceans, squid and fish
349 also exhibited higher median $\delta^{15}\text{N}$ values at La Pérouse (5.2, 9.8, 10.7 and 10.4‰,
350 respectively) compared to MAD-Ridge (3.7, 8.8, 9.5 and 10.0‰, respectively) (Fig. 4) but
351 differences were not statistically significant ($p > 0.05$ each). The $\delta^{13}\text{C}$ values of crustaceans,
352 squid and mesopelagic fish encompassed the same narrow range at La Pérouse and MAD-
353 Ridge (-17.2 to -21.0‰ and -17.1 to -21.1‰, respectively). Gelatinous salps and pyrosomes
354 exhibited $\delta^{13}\text{C}$ values of -18.2 to -21.7‰ at La Pérouse and -19.0 to -23.5‰ at MAD-Ridge.

355 3.3 Relationships between $\delta^{13}\text{C}$ and $\delta^{15}\text{N}$ values

356 Ascending the foodweb, from POM-Surf to mesopelagic fish at La Pérouse and MAD-Ridge
357 seamounts, there was a general increase in $\delta^{13}\text{C}$ and $\delta^{15}\text{N}$ values (Figs. 3 and 4). There was a
358 significantly positive correlation between $\delta^{13}\text{C}$ and $\delta^{15}\text{N}$ values of all sampled components of
359 the foodweb at La Pérouse and MAD-Ridge seamount stations ($p < 0.05$), with Spearman
360 correlation coefficients of $r= 0.74$ and $r= 0.51$, respectively.

361 3.4 Trophic levels at La Pérouse and MAD-Ridge seamounts

362 Albeit small differences in trophic positions between the two methods, they both identified
363 the same organisms at the lowest (leptocephali and gelatinous organisms) and highest
364 (mesopelagic fish excluding leptocephali, and squid) trophic positions. For comparison with
365 other studies published in the region (Ménard et al., 2014; Annasawmy et al., 2018), the
366 additive trophic enrichment model with fixed enrichment factor, TPA, (Eq. 1), is explored in
367 further details.

368 Leptocephali showed estimated TL values (from Eq. 1) of 1.9 and 1.8 at both La Pérouse and
369 MAD-Ridge, respectively (Fig. 5). TL values of crustaceans fell between 2.7 (La Pérouse and
370 MAD-Ridge: *Funchalia* sp.) and 3.7 (La Pérouse: Sergestidae; MAD-Ridge: Oplophoridae).
371 Squid had TL values of 3.6 (*Abraliopsis* sp.) and 4.0 (*Histioteuthis* spp.) at La Pérouse. At
372 MAD-Ridge seamount, smaller-sized nektonic squid (26-111 mm DML) displayed TL values
373 of 3.2 (Enoploteuthidae) and 3.6 (*Abraliopsis* sp.), and larger-sized nektonic squid (365-367
374 mm DML) had TL values of 4.0 (*Histioteuthis* spp.) and 4.8 (*O. bartramii*). TL values of fish
375 (excluding leptocephali) fell between 3.2 (*C. warmingii*) and 4.5 (*C. atrata*) at La Pérouse
376 and between 2.6 (*Decapterus macarellus*) and 4.4 (*Stomias longibarbat*) at MAD-Ridge
377 (Fig. 5). Overall, the TL values of the micronekton broad categories displayed the same range
378 of TL values at both seamounts.

379 3.5 Effect of feeding mode of gelatinous plankton and micronekton on stable isotope values

380 The trophic groups identified by cluster analyses are in general agreement with the postulated
381 feeding habits of the group members at both La Pérouse and MAD-Ridge seamounts,
382 although significant differences exist when individual species are considered. The cluster
383 analyses based on $\delta^{13}\text{C}$ and $\delta^{15}\text{N}$ values identified two main groups, designated I and II, and
384 two subgroups within group I and group II at La Pérouse and MAD-Ridge (Fig. 6). At La
385 Pérouse, Group I included the filter-feeding pyrosomes (IA) and the detritivorous

386 leptocephali (IB) that showed similar $\delta^{13}\text{C}$ values (-21.5 ± 0.2 and $-20.4 \pm 0.5\text{‰}$,
387 respectively) and $\delta^{15}\text{N}$ values (5.2 ± 0.2 and $4.9 \pm 2.1\text{‰}$, respectively). Group IIa compared a
388 single salp specimen ($\delta^{13}\text{C}$: -18.2‰ and $\delta^{15}\text{N}$: 5.9‰) and an omnivorous crustacean
389 *Funchalia* sp. with similar $\delta^{13}\text{C}$ and $\delta^{15}\text{N}$ values (-18.7 ± 0.6 and $7.5 \pm 0.5\text{‰}$, respectively).
390 All other crustaceans having an omnivorous feeding mode displayed greater $\delta^{15}\text{N}$ values
391 ($10.0 \pm 1.1\text{‰}$) and were thus segregated within subgroup IIB along with carnivorous
392 mesopelagic fish and squid (Fig 6). All values are given in mean \pm S.D.

393 At MAD-Ridge, Group I included filter feeding pyrosomes (IA) and salps, and detritivorous
394 leptocephali (IB) which exhibited the most depleted $\delta^{13}\text{C}$ and $\delta^{15}\text{N}$ values relative to
395 omnivorous and carnivorous micronekton (Fig. 6). Group II was subdivided into Group IIA
396 included the squid *O. bartramii*, the fish *Promethichthys prometheus* and *S. longibarbaratus*, all
397 three having carnivorous feeding modes with similar $\delta^{13}\text{C}$ values and the highest $\delta^{15}\text{N}$ values
398 for the greatest sizes. The single large squid *Histioteuthis* spp. (DML: 367 mm) showed a
399 high $\delta^{15}\text{N}$ value of 10.7‰ and a more depleted $\delta^{13}\text{C}$ value of -21.0‰ compared with *O.*
400 *bartramii*, *P. prometheus* and *S. longibarbaratus*. This squid was hence segregated from
401 subgroup IIA. All other omnivorous and carnivorous organisms exhibited lower $\delta^{15}\text{N}$ values
402 (Fig. 6) and were thus included within subgroup IIB. Cluster analyses run on $\delta^{13}\text{C}$ and $\delta^{15}\text{N}$
403 values of micronekton and excluding the outliers salps, pyrosomes, *Funchalia* sp. and
404 leptocephali, also segregated individuals according to their feeding mode at MAD-Ridge ($p <$
405 0.05).

406 3.6 Effect of size of micronekton on $\delta^{15}\text{N}$ values

407 The $\delta^{15}\text{N}$ values of individuals were significantly influenced by their sizes at both La Pérouse
408 ($F_{1,113}=6.70$, $p < 0.05$) and MAD-Ridge ($F_{1,160}= 23.3$, $p < 0.05$), with increasing $\delta^{15}\text{N}$ values
409 as the size of the organisms increased (La Pérouse: $\delta^{15}\text{N}_{\text{gelatinous and micronekton } <100 \text{ mm}} = 8.83 +$

410 $0.02 \times \text{Size}$; MAD-Ridge: $\delta^{15}\text{N}_{\text{gelatinous and micronekton } <100 \text{ mm}} = 7.33 + 0.03 \times \text{Size}$). Eight
411 micronekton species were further selected according to sample size, their common
412 occurrence at both seamounts, their wide body length ranges, differing feeding modes and
413 vertical migration patterns. The $\delta^{15}\text{N}$ values of the selected species *Sigmops elongatus*
414 (carnivore; diel vertical migrator) and *C. warmingii* (omnivore; diel vertical migrator) were
415 significantly influenced by their lengths (Fig. 7a, b, Table 1), with higher $\delta^{15}\text{N}$ values at La
416 Pérouse than at MAD-Ridge. The $\delta^{15}\text{N}$ values of the fish *A. aculeatus* (carnivore, mid-water
417 migrant) and of the crustacean *Funchalia* sp. (omnivore, diel vertical migrator) were
418 significantly influenced by their lengths but were not significantly different between La
419 Pérouse and MAD-Ridge (Fig. 7c, d, Table 1). The mesopelagic fish *D. suborbitalis* and the
420 squid *Abraliopsis* sp. (both carnivores and diel vertical migrators) exhibited the same range of
421 $\delta^{15}\text{N}$ values irrespective of size at La Pérouse and MAD-Ridge (Fig. 7e, f, Table 1). For the
422 same body length, *Abraliopsis* sp. showed higher $\delta^{15}\text{N}$ values at La Pérouse relative to MAD-
423 Ridge (Fig. 7f). Models fitted to *C. sloani* (carnivore, diel vertical migrator) and leptocephali
424 (detritivore, migrant or non-migrant depending on species) were not significant (Fig. 7g, h,
425 Table 1). The detritivorous leptocephali had varied $\delta^{15}\text{N}$ values irrespective of size and
426 irrespective of the sampling location.

427 The $\delta^{15}\text{N}$ values of omnivorous/ carnivorous fish collected in the vicinity of the La Pérouse
428 and MAD-Ridge seamounts and in the southern Mozambique Channel were significantly
429 influenced by individual body size ($F_{3,171} = 10.3$, Adjusted $R^2=13.8$, $p < 0.05$) (Fig. 8a).
430 However, there were no significant influence of body size on the $\delta^{15}\text{N}$ values of seamount
431 flank- and summit-associated fish species *D. suborbitalis* (La Pérouse and MAD-Ridge), *B.*
432 *fibulatum*, *D. knappi* and *C. japonicus* ($F_{1,10} = 0.07$, $p > 0.05$) at MAD-Ridge. These seamount
433 flank- and summit-associated fish species (Annasawmy et al., 2019; Cherel et al., 2020)
434 exhibited minimum and maximum $\delta^{15}\text{N}$ values of 9.8‰ (*B. fibulatum*) and 11.2‰ (*D.*

435 *suborbitalis*) for individuals ranging in size from 38 mm (*D. suborbitalis*) to 328 mm (*C.*
436 *japonicus*) (Fig. 8b). Despite the differing sizes of these seamount flank- and summit-
437 associated fish species, they exhibited an estimated TL value (TPA model) of ~4 at both La
438 Pérouse and MAD-Ridge pinnacles.

439 3.7 Effect of time of day on $\delta^{13}\text{C}$ and $\delta^{15}\text{N}$ values at MAD-Ridge seamount

440 Gelatinous and micronekton organisms sampled at MAD-Ridge exhibited similar $\delta^{13}\text{C}$ values
441 (-19.6 and -19.4‰ respectively) during day and night ($W= 3055.5$, $p > 0.05$). However,
442 individuals collected during daylight showed higher median $\delta^{15}\text{N}$ values (9.22‰) than those
443 collected at night (8.12‰) ($W= 4757.5$, $p < 0.05$).

444 3.8 Seamount effect on $\delta^{13}\text{C}$ and $\delta^{15}\text{N}$ values of omnivorous/carnivorous fish

445 The $\delta^{13}\text{C}$ and $\delta^{15}\text{N}$ values of omnivorous/carnivorous fish had overlapping ranges at La
446 Pérouse flank and vicinity stations as well as overlapping ranges at MAD-Ridge flank,
447 summit and vicinity and Mozambique Channel stations (Fig. 9). There were no significant
448 differences in $\delta^{13}\text{C}$ ($W= 1619$, $p > 0.05$) of omnivorous/carnivorous fish collected between
449 flank stations and the vicinity of La Pérouse seamount, whereas a significant difference was
450 observed for $\delta^{15}\text{N}$ values between flank (median: 10.1‰) and vicinity (median: 10.8‰)
451 stations ($W= 1876$, $p < 0.05$). There was also no significant difference in $\delta^{13}\text{C}$ values (KW,
452 $H= 1.0$, $df= 2$, $p > 0.05$) of omnivorous/carnivorous fish collected in the southern
453 Mozambique Channel, the vicinity, flank and summit of MAD-Ridge. However, there was a
454 significant difference in $\delta^{15}\text{N}$ values (KW, $H= 8.5$, $df= 3$, $p > 0.05$) of
455 omnivorous/carnivorous fish collected from the southern Mozambique Channel (median:
456 10.6‰) and in the vicinity of MAD-Ridge (median: 10.0‰).

457

458 4. Discussion

459 To our knowledge, this study is the first to investigate trophic interactions of mesopelagic
460 communities at La Pérouse and MAD-Ridge seamounts using $\delta^{13}\text{C}$ and $\delta^{15}\text{N}$ stable isotopes.
461 The foodweb components POM-Surf, POM-Fmax, zooplankton, gelatinous organisms and 42
462 and 49 taxonomic groups of micronekton were identified at La Pérouse and MAD-Ridge,
463 respectively. Despite the low sample sizes for some species, our datasets provide a first
464 overview of the trophic relationships of micronekton at both seamounts.

465 4.1 Sampling bias and constraints

466 The full suite of foodweb components could not be sampled at both seamounts because of
467 trawl gear catchability, selectivity and net avoidance of some species of squid and larger fish.
468 Stable isotopes also have numerous limitations in the extent to which they can be used to
469 elucidate complex foodweb dynamics. Isotopic baselines vary seasonally and spatially
470 (Ménard et al., 2014), and organisms or tissues within a single individual may incorporate the
471 isotopic signal of their diets at varying rates, thereby influencing the stable isotope values of
472 individuals (Martínez Del Rio et al., 2009). The use of pelagic tunicates as isotopic baseline
473 in TL calculations can also be problematic because pelagic tunicates may be members of an
474 alternate microbial foodweb (Pakhomov et al., 2019). There have been concerns in previous
475 studies of the inappropriate use of fixed discrimination factors for trophic position
476 estimations (Caut et al., 2009; Hussey et al., 2014). However, as shown in Olivar et al. (2019)
477 for myctophid species, and in our study for zooplankton and micronekton, the methods for
478 trophic position estimates maintained the essential differences among all species.
479 Furthermore, the $\delta^{15}\text{N}$ values of gelatinous plankton and micronekton were significantly
480 different between day and night samples at MAD-Ridge. This was probably due to the
481 sampling depth, because night-time samples were collected in the shallow, intermediate and
482 deep layers, whereas daylight samples were collected mostly in the deep layer (apart from
483 two leptocephali collected in the shallow depth category). Previous studies found higher $\delta^{15}\text{N}$

484 and $\delta^{13}\text{C}$ values with depth, which have been linked to the increase of $\delta^{15}\text{N}$ in POM with
485 depth (Kolasinski et al., 2012; Fanelli et al., 2013). However, as the IYGPT net had no
486 closing device, the effect of sampling depth on $\delta^{13}\text{C}$ and $\delta^{15}\text{N}$ values of individuals could not
487 be investigated further.

488 Recent studies have cautioned against the use of a fixed additive nitrogen enrichment factor
489 of $\sim 3.2\text{--}3.4\text{‰}$ that is commonly used to estimate the trophic position of an organism relative
490 to its diet. Caut et al. (2009) showed that the consumer taxonomic group and consumer tissue
491 significantly affect the discrimination factor used in trophic level calculations, and Hussey et
492 al. (2014) stressed that the enrichment between consumers and their primary prey items
493 becomes narrower in the upper parts of a food chain. Bastos et al. (2017) developed a novel
494 method using food-specific trophic discrimination factors to estimate trophic positions of
495 omnivorous fish given that plant-based and animal-based materials in diets are not
496 assimilated in the same manner. Olivar et al. (2019) observed small variations in trophic level
497 calculations of mesopelagic fish when using alternative models to estimate trophic positions.
498 However, those authors also concluded that the important differences among species are
499 retained by all trophic models, similarly to the findings of this study.

500 4.2 Trophic interactions at La Pérouse and MAD-Ridge seamounts

501 Particulate organic matter collected at the surface generally consists of phytoplankton,
502 bacteria, faecal pellets and detritus (Riley, 1971; Saino & Hattori, 1987; Fabiano et al., 1993;
503 Dong et al., 2010; Liénart et al., 2017). The $\delta^{13}\text{C}$ values of POM (collected at the surface and
504 at the Fmax depth) were different at the La Pérouse and MAD-Ridge seamounts. $\delta^{13}\text{C}$
505 baselines can be affected by various processes such as latitude, nutrient source, depth, ocean
506 mixing and primary productivity (Fry, 2006). Research has found that chlorophyll *a*
507 concentrations explained the variability in POM $\delta^{13}\text{C}$ values within the EAFR province but

508 not in the ISSG (Annasawmy et al., 2018). Surface chlorophyll *a* concentrations at MAD-
509 Ridge (within the EAFR province) was greater than at La Pérouse (within the ISSG) all year
510 round (Annasawmy et al., 2019), likely a result of terrestrial input of nutrients from the
511 Madagascar landmass, upwelling events on the shelf to the south of Madagascar
512 (Ramanantsoa et al., 2018), offshore advection of this shelf productivity through cross-shelf
513 transport (Noyon et al., 2018) and vertical mixing in the mesoscale eddy system over MAD-
514 Ridge (De Ruijter et al., 2004; Vianello et al., 2020). High levels of photosynthetic rate
515 (currently occurring at the south Madagascar upwelling and being transported south), would
516 induce higher $\delta^{13}\text{C}$ POM values at MAD-Ridge compared with the oligotrophic La Pérouse
517 (Fry, 1996; Savoye et al., 2003). Surface POM at MAD-Ridge might have possibly been both
518 of marine and terrestrial origin, yielding higher $\delta^{13}\text{C}$ values relative to surface POM at La
519 Pérouse, which might have consisted of phytoplankton with no terrestrial POM input.

520 The $\delta^{13}\text{C}$ - $\delta^{15}\text{N}$ correlations of all foodweb components were not relatively strong at the La
521 Pérouse and MAD-Ridge seamounts ($r = 0.74$ and 0.51 respectively) at the times of the
522 cruises. A strong correlation during periods of high productivity would have supported the
523 hypothesis of a unique and isotopically homogeneous pelagic food source (Fanelli et al.,
524 2013; Papiol et al., 2013; Preciado et al., 2017), i.e. a single source of carbon for plankton
525 (Fanelli et al., 2009). The relatively weaker correlation observed in our study suggests a wide
526 array of sources of production sustaining the different assemblages once the main input from
527 surface production has decreased (Fanelli et al., 2011a, b; Papiol et al., 2013), or exploitation
528 of organic matter at different stages of degradation from fresh phytodetritus to highly
529 recycled (Fanelli et al., 2009), or refractory materials such as chitin from copepod
530 exoskeleton becoming abundant in sinking marine snow or inorganic carbonates (Polunin et
531 al., 2001). This would be the case in low productive environments such as the ISSG, where
532 production at La Pérouse would be reduced in September (Annasawmy et al., 2019) and thus

533 zooplankton would have to expand their food spectrum, as demonstrated by the larger span of
534 their niche widths over the $\delta^{13}\text{C}$ range. Alternatively, the $\delta^{13}\text{C}$ - $\delta^{15}\text{N}$ correlations could reflect
535 temporal variations in the baseline isotope values coupled with varying rates of isotopic
536 incorporation (Fanelli et al., 2009, 2011b, 2013). Higher trophic level organisms such as large
537 crustaceans and fish reportedly do not show seasonal patterns in their isotope values owing to
538 their much slower tissue turnover rates (Polunin et al., 2001). Additional seasonal studies are
539 required to investigate POM and resulting zooplankton $\delta^{13}\text{C}$ and $\delta^{15}\text{N}$ signatures in July when
540 surface oceanic phytoplankton production is enhanced within the ISSG and EAFR provinces
541 (Annasawmy et al., 2018, 2019).

542 Among the mesopelagic organisms sampled, gelatinous plankton exhibited the lowest trophic
543 level (~ 2), crustaceans showed an intermediate trophic level (~ 3), and smaller squid and
544 mesopelagic fish exhibited TL values between 3 and 4, as estimated from the TPA method.
545 Assuming a fixed and additive trophic fractionation of 3.2‰ (for comparison with other
546 SWIO studies), the overall range of $\delta^{15}\text{N}$ values implied a two-step (3 trophic levels) and
547 three-step (four trophic levels) pelagic food chain at La Pérouse and MAD-Ridge seamounts,
548 respectively. Unfortunately, no top predators were sampled during these cruises to provide
549 information on higher trophic level organisms. Earlier studies within the EAFR province,
550 showed swordfish *Xiphias gladius* collected off the coast of Madagascar to have a TL of ~ 4.7
551 ($\delta^{15}\text{N}$: $14.0 \pm 0.59\text{‰}$). Specimens collected within the ISSG province had a TL of ~ 5.2 ($\delta^{15}\text{N}$:
552 $15.1 \pm 0.36\text{‰}$) (Annasawmy et al., 2018). Several authors described the number of trophic
553 levels averaging between four and six in marine ecosystems, from primary consumers to top
554 predators, and appearing higher in coastal environments, reefs and shelves and lower in
555 oceanic upwelling systems (Arreguín-Sánchez et al., 1993; Browder, 1993; Christensen &
556 Pauly, 1993; Bulman et al., 2002). Similar to those studies, it seems that both La Pérouse and
557 MAD-Ridge seamounts exhibit trophic levels typical of oceanic systems, although small

558 variations may exist in the $\delta^{13}\text{C}$ and $\delta^{15}\text{N}$ values of an organism's tissues according to various
559 environmental, behavioural and physiological factors (Ménard et al., 2014; Annasawmy et
560 al., 2018).

561 4.3 Influence of feeding mode and size on $\delta^{13}\text{C}$ and $\delta^{15}\text{N}$ values

562 The trophic guilds established at La Pérouse and MAD-Ridge seamounts were segregated in
563 terms of $\delta^{13}\text{C}$ and $\delta^{15}\text{N}$ values, from depleted (detritivores and filter-feeders) to enriched
564 (omnivores and carnivores) isotope values, highlighting the fact that these trophic guilds
565 consist of species that exploit distinct classes of resources (Bulman et al., 2002; Papiol et al.,
566 2013; Choy et al., 2016). The large range of $\delta^{13}\text{C}$ values (~ 17 to -23‰) when gelatinous
567 organisms are considered together with crustaceans, squid and mesopelagic fish suggests that
568 these organisms exploit different sources of production, thus giving rise to different trophic
569 pathways (Ménard et al., 2014). Gelatinous filter feeders such as salps and pyrosomes ingest
570 a variety of suspended particles (Harbou, 2009; Conley, 2017) and leptocephali include a
571 wide range of species feeding on detrital material (Otake et al., 1993) such as larvacean
572 houses and faecal pellets (Lecomte-Finiger et al., 2004; Feunteun et al., 2015) and hence
573 exhibited depleted $\delta^{13}\text{C}$ values relative to other micronekton broad categories. Species
574 depleted in ^{13}C reportedly feed near the base of the food chain and are closely associated with
575 plankton relative to fish with higher $\delta^{13}\text{C}$ values (Polunin et al., 2001).

576 Crustacean taxa were at intermediate trophic levels at both seamounts, below that of strict
577 carnivores and above that of detritivores or filter-feeding organisms. Some species of
578 crustaceans would prey on chaetognaths (Heffernan & Hopkins, 1981), molluscs, olive-green
579 debris containing phytoplankton and protists (Hopkins et al., 1994), and they would share
580 common food sources with mesopelagic fish by foraging on copepods, decapods and
581 euphausiids (Fanelli et al., 2009). Similar to previous studies conducted in the SWIO

582 (Ménard et al., 2014; Annasawmy et al., 2018), crustaceans exhibited overlapping isotopic
583 niches with carnivorous mesopelagic fish and squid at both seamounts. The narrow range of
584 $\delta^{13}\text{C}$ values and the greater overlap of isotopic niches between crustaceans and carnivorous
585 squid and mesopelagic fish at both seamounts might suggest some degree of similarity in the
586 diet components with low level of resource partitioning and a high level of competition
587 among these broad categories (Fanelli et al., 2009) or alternatively, different diets but with
588 prey items having similar isotopic compositions.

589 Whereas lower trophic level components, POM-Fmax and zooplankton showed significantly
590 different and higher $\delta^{15}\text{N}$ values at MAD-Ridge relative to La Pérouse (most likely because
591 of differing productivity and fast turnover rate of these organisms), higher trophic level
592 components such as crustaceans, squid and fish showed no significant differences in their
593 $\delta^{15}\text{N}$ values between the two seamounts. There are several hypotheses for similar isotopic
594 signatures of higher trophic levels when baseline levels differ. First, the sampled organisms
595 might not have had time to incorporate the isotopic composition of their most recent diets,
596 especially if transient productivity bouts had impacted the density or composition of their
597 diet. Whereas some studies reported tissue turnover rates of ~0.1-0.2% per day in deep-sea
598 fish (Hesslein et al., 1993), other studies showed a lack of tissue turnover information in more
599 specific mesopelagic families including Myctophidae and Stomiidae (Choy et al., 2012).
600 Second, the difference in the $\delta^{15}\text{N}$ values of POM and zooplankton observed at La Pérouse
601 and MAD-Ridge, although significant, may have been too negligible to be reflected in the
602 $\delta^{15}\text{N}$ values of higher trophic levels. Third, the number of squid and crustacean specimens
603 analysed for stable isotopes might not be large enough to reflect the full diversity in the
604 isotopic signatures, and hence the apparent lack of variations in $\delta^{15}\text{N}$ values for these
605 individuals between the two seamounts. Finally, as a result of movements, zooplankton
606 grazers and subsequent trophic levels might have fed on prey components that are not those

607 sampled in the water column, leading to a mismatch in isotopic signatures between lower and
608 higher trophic levels.

609 In this study, $\delta^{15}\text{N}$ values of micronekton were correlated to body size. This phenomenon was
610 observed in various organisms such as phytoplankton, zooplankton, decapods and fish and
611 across numerous studies (Sholto-Douglas et al., 1991; France et al., 1998; Waite et al., 2007;
612 Ventura & Catalan, 2008; Hirsch & Christiansen, 2010; Choy et al., 2012, 2015; Papiol et al.,
613 2013) and is probably attributable to size-related predation. As organisms grow in size, they
614 can feed farther up the foodweb on larger prey with greater $\delta^{15}\text{N}$ values (Parry, 2008; Ménard
615 et al., 2014). For those species whose $\delta^{15}\text{N}$ values (*S. elongatus*, *C. warmingii* and
616 *Abraliopsis* sp.) were significantly influenced by size, their $\delta^{15}\text{N}$ values were greater (around
617 1‰ difference) at La Pérouse than at MAD-Ridge for the same body lengths. As suggested in
618 Parry (2008), if the $\delta^{15}\text{N}$ values, and hence the TL of an organism, are influenced by size,
619 then the $\delta^{15}\text{N}$ signal will also depend on baseline values and the variables that affect an
620 organism's size such as feeding mode, growth rate, body condition and available prey items.
621 As $\delta^{15}\text{N}$ values of POM and zooplankton were higher at MAD-Ridge than at La Pérouse, we
622 hypothesize that those intermediate TLs at the oligotrophic La Pérouse seamount had a
623 different trophic functioning, with the diet of those species being based on a larger proportion
624 of higher TL prey than at MAD-Ridge.

625 Body size did not have an effect on $\delta^{15}\text{N}$ values of leptocephali which encompass a wide
626 range of species having a detritivorous and opportunistic feeding mode at both seamounts.
627 Such lack of effect was also observed for *C. sloani* individuals ranging in size from 66 to 184
628 mm at La Pérouse and from 77 to 199 mm at MAD-Ridge. These individuals are semi-
629 migrants, caught in deep and intermediate trawls during both day and night. Individuals 45-
630 178 mm long feed on myctophids and other fish species (Utrecht et al., 1987; Butler et al.,
631 2001) with prey items being more than 63% of their own length (Clarke, 1982). Smaller

632 individuals were reported to feed on euphausiids (Butler et al., 2001). Our trawls failed to
633 capture smaller *C. sloani* individuals which may have had a different diet and possibly
634 different $\delta^{15}\text{N}$ values relative to larger individuals. There might also be a trophic plateau
635 whereby subsequent increases in trophic position with size are not possible due to physical
636 constraints on the organism or lack of appropriate prey of higher trophic levels, as was
637 observed with *O. bartramii* specimens from the Central North Pacific (Parry, 2008).

638 4.4 Seamount effect on $\delta^{13}\text{C}$ and $\delta^{15}\text{N}$ values of fish species

639 Omnivorous/carnivorous fish sampled in the southern Mozambique Channel exhibited
640 slightly enriched $\delta^{15}\text{N}$ values relative to those sampled in the vicinity of the MAD-Ridge
641 seamount. Productivity in the southern Mozambique Channel may be both entrained from the
642 African landmass and locally generated within mesoscale eddies, hence leading to enhanced
643 chlorophyll *a* concentration, micronekton abundances and enriched $\delta^{15}\text{N}$ values within tissues
644 of micronekton (Tew-Kai & Marsac, 2009; Annasawmy et al., 2018). For an increase in
645 phytoplankton biomass to take place at the seamounts, physical processes leading to retention
646 (e.g. Taylor columns trapping a body of water), enrichment (e.g. localised upwelling and
647 uplift of nutrients) and concentration of productivity must co-occur (Bakun, 2006). However,
648 as seen at La Pérouse and MAD-Ridge seamounts, the current speeds were too strong during
649 the cruise, and the seamount structures unfavourable for Taylor column formation and for
650 significant retention and assimilation of productivity (Annasawmy et al., 2020). This would
651 have inhibited any subsequent energy transfer to higher trophic levels, potentially explaining
652 the lack of differences in $\delta^{15}\text{N}$ values between the seamount and the area not influenced by
653 the seamount.

654 Seamount-associated fish species *D. suborbitalis*, *B. fibulatum* and *C. japonicus* (Annasawmy
655 et al., 2019; Cherel et al., 2020), sampled at the summit and on the flanks of MAD-Ridge

656 showed similar $\delta^{13}\text{C}$, $\delta^{15}\text{N}$ and TL values irrespective of their size, similarly to *D.*
657 *suborbitalis* sampled at La Pérouse. This most likely reflects similar food sources at the
658 summit and flanks of both pinnacles or ingestion of different prey items having similar
659 isotopic composition. These fish may associate with the La Pérouse and MAD-Ridge
660 summits and flanks owing to enhanced availability of prey and/or the quiescent shelters
661 offered by the topography (Annasawmy et al., 2019). All seamount-associated fish
662 individuals collected on the summit and flanks of La Pérouse and MAD-Ridge with the
663 IYGPT net were adults, previously reported to prey on copepods (Go, 1986; Olivar et al.,
664 2019; Vipin et al., 2018) and chaetognaths (Appelbaum, 1982), organisms present in similar
665 proportions on and away from both seamounts (Noyon et al., 2020).

666 Although $\delta^{13}\text{C}$ and $\delta^{15}\text{N}$ values may depend on a range of factors, there were few differences
667 between $\delta^{13}\text{C}$ and $\delta^{15}\text{N}$ values of mesopelagic fish sampled at La Pérouse and MAD-Ridge
668 and those collected in the Indian Ocean, within the oligotrophic ISSG province (*A. aculeatus*
669 $\delta^{13}\text{C}$ and $\delta^{15}\text{N}$ values: -18.6 and 9.5‰, *C. sloani*: -18.1 and 9.5‰, and *L. gemellarii*: -18.5
670 and 9.9‰; Annasawmy et al., 2018) and the western Mozambique Channel (*A. aculeatus*: -
671 18.4 and 10.0‰ and *L. gemellarii*: -18.4 and 11.1‰; Annasawmy et al., 2018). Even though
672 mesopelagic fish exhibit small variations in their $\delta^{13}\text{C}$ and $\delta^{15}\text{N}$ values across different
673 studies in various oceanic environments, they generally occupy trophic positions between 2
674 and 4, irrespective of the approach used to estimate trophic positions (Fanelli et al., 2011b;
675 Choy et al., 2012, 2015, 2016; Colaço et al., 2013; Ménard et al., 2014; Valls et al., 2014a,b;
676 Denda et al., 2017; Annasawmy et al., 2018; Olivar et al., 2019). Despite the possible bias
677 induced by the different time-scales in sampling (Mill et al., 2008), within a stable isotope
678 approach, the trophic positions of mesopelagic fish across numerous studies confirmed
679 similar dietary patterns and food sources with similar isotopic compositions. Hence, these

680 mesopelagic fish species by their opportunistic feeding mode may play a similar trophic role
681 across different environments (Olivar et al., 2019).

682 **Concluding Remarks**

683 This study has shown that despite the different productivity at the two shallow seamounts and
684 the significant differences in lower trophic level $\delta^{13}\text{C}$ and $\delta^{15}\text{N}$ values, crustaceans, smaller-
685 sized squid and mesopelagic fish, because of their varied feeding modes, occupy trophic
686 positions between 3 and 4. Specimen size had an influence on the $\delta^{15}\text{N}$ values of most
687 individuals, although that also depended on the life strategy and feeding mode of the species
688 considered. The $\delta^{13}\text{C}$ and $\delta^{15}\text{N}$ values of mesopelagic organisms sampled during both cruises
689 reflected those of typical oceanic systems and the seamounts did not seem to have any impact
690 on the overall isotopic signatures of the mesopelagic taxa sampled. However, the few
691 seamount-associated/resident fish sampled showed similar $\delta^{15}\text{N}$ values and trophic levels
692 irrespective of their size at the summits and flanks of the pinnacles. La Pérouse and MAD-
693 Ridge seamounts may hence be important foraging grounds for the few taxa that
694 preferentially associate with their slopes and summits, and thus benefit from the varied
695 habitat types that the seamounts offer compared to the open ocean environment.

696

697 **Acknowledgements**

698 We acknowledge the work carried out by the scientific/non-scientific staff on board the RV
699 *Antea* for collection of samples at La Pérouse and MAD-Ridge seamounts. We also thank
700 colleagues at the Plateau Chimie/ Pole Technique MARBEC (Sète, France) and the Pôle de
701 Spectrométrie Océan (Plouzané, France) for providing support with the stable isotope
702 analyses. This study was mainly supported by the Flotte Océanographique Française (French
703 Oceanographic Fleet) and IRD in relation to the logistics of the RV *Antea*. Additional

704 funding was also received from Région Reunion (Réunion Regional Council) for the La
705 Pérouse cruise, and from the Fonds Français pour l'Environnement Mondial (FFEM) as part
706 of the FFEM-SWIO project on Areas Beyond National Jurisdiction (ABNJ) of the South
707 West Indian Ocean for the MAD-Ridge cruise. The first author was the beneficiary of a
708 doctoral bursary granted by the Institut de Recherche pour le Développement (IRD, France)
709 and the ICEMASA French-South African International Laboratory.

References

- Annasawmy, P., Ternon, J.F., Marsac, F., Cherel, Y., Béhagle, N., Roudaut, G., Lebourges-Dhaussy, A., Demarcq, H., Moloney, C.L., Jaquemet, S., Ménard, F., 2018. Micronekton diel migration, community composition and trophic position within two biogeochemical provinces of the South West Indian Ocean: Insight from acoustics and stable isotopes. *Deep Sea Research Part I: Oceanographic Research Papers*. 138, 85–97. <https://doi.org/10.1016/j.dsr.2018.07.002>
- Annasawmy, P., Ternon, J-F., Cotel, P., Demarcq, H., Cherel, Y, Romanov, E., Roudaut, G., Lebourges-Dhaussy, A., Ménard, F., Marsac, F. 2019. Micronekton distribution and assemblages at two shallow seamounts in the south-western Indian Ocean: Insights from acoustics and mesopelagic trawl data. *Progress in Oceanography*-accepted.
- Annasawmy, P., Ternon, J-F., Lebourges-Dhaussy, A., Roudaut, G., Herbette, S., Ménard, F., Cotel., P., Marsac, F., 2020. Micronekton distribution as influenced by mesoscale eddies, Madagascar shelf and shallow seamounts in the south-western Indian Ocean: An acoustic approach. *Deep-Sea Res. II*, this issue.
- Appelbaum, S., 1982. Studies on food organisms of pelagic fishes as revealed by the 1979 North Atlantic Eel Expedition. *Helgoländer Meeresuntersuchungen*. 35, 357–367. <https://doi.org/10.1007/BF02006143>
- Arreguín-Sánchez, F., Valero-Pacheco, E., Chávez, E.A., 1993. A Trophic Box Model of the Coastal Fish Communities of the Southwestern Gulf of Mexico. In V. Christensen and D. Pauly (Eds) *Trophic Models of Aquatic Ecosystems*. ICLARM Conference Proceedings, 26: 390.
- Bakun, A., 2006. Fronts and eddies as key structures in the habitat of marine fish larvae: opportunity, adaptive response and competitive advantage. *Sci. Mar.* 70, 105–122. <https://doi.org/10.3989/scimar.2006.70s2105>
- Bastos, R.F., Corrêa, F., Winemiller, K.O., Garcia, A.M., 2017. Are you what you eat? Effects of trophic discrimination factors on estimates of food assimilation and trophic position with a new estimation method. *Ecological Indicators*. 75: 234-241. <http://dx.doi.org/10.1016/j.ecolind.2016.12.007>
- Bernal, A., Olivar, M.P., Maynou, F., Fernández de Puellas, M.L., 2015. Diet and feeding strategies of mesopelagic fishes in the western Mediterranean. *Progr. Oceanogr.* 135, 1-17. <https://doi.org/10.1016/j.pocean.2015.03.005>
- Bertrand, A., Bard, F.X. Josse, E., 2002. Tuna food habits related to the micronekton distribution in French Polynesia. *Mar Biol.* 140: 1023-1037. DOI: 10.1007/s00227-001-0776-3
- Bianchi, D., Stock, C., Galbraith, E.D., Sarmiento, J.L., 2013. Diel vertical migration: Ecological controls and impacts on the biological pump in a one-dimensional ocean model. *Global Biogeochem. Cycles*. 27: 478-491. DOI: 10.1002/gbc.20031
- Birkley, S.-R., Gulliksen, B., Feeding Ecology in Five Shrimp Species (Decapoda, Caridea) from an Arctic Fjord (Isfjorden, Svalbard), with Emphasis on *Sclerocrangon boreas* (Phipps, 1774).
- Bodin, N., Budzinski, H., Le Ménach, K., Tapie, N., 2009. ASE extraction method for simultaneous carbon and nitrogen stable isotope analysis in soft tissues of aquatic organisms. *Analytica Chimica Acta*. 643: 54-60. DOI: 10.1016/j.aca.2009.03.048
- Brodeur, R., Yamamura, O., 2005. PICES Scientific Report No. 30 Micronekton of the North Pacific. PICES Scientific Report, Sidney B.C., Canada, pp. 1-115.

- Browder, J.A., 1993. A pilot model of the Gulf of Mexico continental shelf. In V. Christensen and D. Pauly (Eds) Trophic Models of Aquatic Ecosystems. ICLARM Conference Proceedings. 26: 390.
- Bulman, C.M., He, X., Koslow, J.A., 2002. Trophic ecology of the mid-slope demersal fish community off southern Tasmania, Australia. *Mar. Freshwater Res.* 53: 59-72. DOI: 10.1071/MF01057
- Butler, M., Bollens, S.M., Burkhalter, B., Madin, L.P., Horgan, E., 2001. Mesopelagic fishes of the Arabian Sea: distribution, abundance and diet of *Chauliodus pammelas*, *Chauliodus sloani*, *Stomias aznis*, and *Stomias nebulosus*. *Deep-Sea Res. II.* 48: 1369-1383.
- Carmo, V., Sutton, T., Menezes, G., Falkenhaus, T., Bergstad, O.A., 2015. Feeding ecology of the Stomiiformes (Pisces) of the northern Mid-Atlantic Ridge. 1. The Sternoptychidae and Phosichthyidae. *Prog. Oceanogr.* 130: 172-187. <https://doi.org/10.1016/j.pocean.2014.11.003>
- Catul, V., Gauns, M., Karuppasamy, P.K., 2011. A review of mesopelagic fishes belonging to family Myctophidae. *Rev. Fish Biol. Fisheries.* 21: 339-354. DOI: 10.1007/s11160-010-9176-4
- Caut, S., Angulo, E., Courchamp, F., 2009. Variation in discrimination factors ($\Delta^{15}\text{N}$ and $\Delta^{13}\text{C}$): the effect of diet isotopic values and applications for diet reconstruction. *Journal of Applied Ecology.* 46: 443-453. DOI: 10.1111/j.1365-2664.2009.01620.x
- Cherel, Y., Fontaine, C., Richard, P., Labat, J.-P., 2010. Isotopic niches and trophic levels of myctophid fishes and their predators in the Southern Ocean. *Limnol. Oceanogr.* 55, 324–332. <https://doi.org/10.4319/lo.2010.55.1.0324>
- Cherel, Y., Romanov, E.V., Annasawmy, P., Thibault, D., Ménard, F., 2020. Micronektonic fish species over three seamounts in the southwestern Indian Ocean. *Deep-Sea Res. II.* <https://doi.org/10.1016/j.dsr2.2020.104777>
- Choy, C.A., Davison, P.C., Drazen, J.C., Flynn, A., Gier, E.J., Hoffman, J.C., McClain-Counts, J.P., Miller, T.W., Popp, B.N., Ross, S.W., Sutton, T.T., 2012. Global trophic position comparison of two dominant mesopelagic fish families (Myctophidae, Stomiidae) using amino acid nitrogen isotopic analyses. *PLoS One.* 7(11): e50133. DOI: 10.1371/journal.pone.0050133
- Choy, C.A., Popp, B.N., Hannides, C.C.S., Drazen, J.C., 2015. Trophic structure and food resources of epipelagic and mesopelagic fishes in the North Pacific Subtropical Gyre ecosystem inferred from nitrogen isotopic compositions. *Limnol. Oceanogr.* 60: 1156-1171.
- Choy, C.A., Wabnitz, C.C.C., Weijerman, M., Woodworth-Jefcoats, P.A., Polovina, J.J., 2016. Finding the way to the top: how the composition of oceanic mid-trophic micronekton groups determines apex predator biomass in the central North Pacific. *Mar. Ecol. Prog. Ser.* 549: 9-25. DOI: 10.3354/meps11680
- Christensen, V., Pauly, D., 1993. Flow Characteristics of Aquatic Ecosystems. In V. Christensen and D. Pauly (Eds) Trophic Models of Aquatic Ecosystems. ICLARM Conference Proceedings. 26: 390.
- Clarke, M.R., Lu, C.C., 1975. Vertical distribution of cephalopods at 18°N 25°W in the North Atlantic. *J. mar. biol. Ass.* 55: 165-182. <https://doi.org/10.1017/S0025315400015812>
- Clarke, T.A., 1982. Feeding habits of stomiatoid fishes from Hawaiian waters. *Fishery Bulletin.* 80(2): 287-304.
- Clarke, K., Warwick, R., 2001. Change in Marine Communities: An Approach to Statistical Analysis and Interpretation. PRIMER-E Ltd: Plymouth, United Kingdom.
- Clark, M.R., Vinnichenko, V.I., Gordon, J D M , Beck-Bulat, G..Z., Kukharev, N. N., and Kakora, A.F., 2007. Large-scale distant-water trawl fisheries on seamounts. In:

- Pitcher, T. J., Morato, T., Hart, P. J. B., Clark, M. R., Haggan, N., & Santos, R. S. (Eds.). *Seamounts: Ecology, Fisheries & Conservation*. Blackwell Publishing. 361-399.
- Colaço, A., Giacomello, E., Porteiro, F., Menezes, G.M., 2013. Trophodynamic studies on the Condor seamount (Azores, Portugal, North Atlantic). *Deep-Sea Res. Part II: Topical Studies in Oceanography*. 98: 178–189. <https://doi.org/10.1016/j.dsr2.2013.01.010>
- Conley, K.P., 2017. *Mechanics and Selectivity of filtration by tunicates*. PhD thesis, University of Oregon, USA.
- Cresson, P., Ruitton, S., Fontaine, M-F., Harmelin-Vivien, M., 2012. *Marine Pollution Bulletin*. 1112-1121. <http://dx.doi.org/10.1016/j.marpolbul.2012.04.003>
- Dalpadado, P., Gjøsæter, J., 1988. Feeding ecology of the lanternfish *Benthosema pterotum* from the Indian Ocean. *Mar. Biol.* 99: 555-567.
- Daly, R., Froneman, P.W., Smale, M.J., 2013. Comparative Feeding Ecology of Bull Sharks (*Carcharhinus leucas*) in the Coastal Waters of the Southwest Indian Ocean Inferred from Stable Isotope Analysis. *PLoS ONE* 8(10): e78229. doi:10.1371/journal.pone.0078229
- Danckwerts, D.K., McQuaid, C.D., McGregor, G.K., Dwight, R., Le Corre, M., Jaquemet, S., 2014. Biomass consumption by breeding seabirds in the western Indian Ocean: indirect interactions with fisheries and implications for management. *ICES Journal of Marine Science*. 71(9): 2589-2598. DOI: 10.1093/icesjms/fsu093
- Davison, P. C., Koslow, J. A., Kloser, R. J., 2015. Acoustic biomass estimation of mesopelagic fish: backscattering from individuals, populations, and communities. *ICES Jour. Mar. Sci.* 72(5), 1413-1424. <https://doi.org/10.1093/icesjms/fsv023>
- De Forest, L., Drazen, J., 2009. The influence of a Hawaiian seamount on mesopelagic micronekton. *Deep-Sea Res. I*. 56: 232-250. DOI: 10.1016/j.dsr.2008.09.007
- Del Giorgio, P.A., Duarte, C.M., 2002. Respiration in the open ocean. *Nature*. 420: 379-384.
- Denda, A., Stefanowitsch, B., Christiansen, B., 2017. From the epipelagic zone to the abyss: Trophic structure at two seamounts in the subtropical and tropical Eastern Atlantic-Part I zooplankton and micronekton. *Deep Sea Res. Part I*. 130: 63-77.
- De Ruijter, W.P.M., Aken, H.M. van, Beier, E.J., Lutjeharms, J.R.E., Matano, R.P., Schouten, M.W., 2004. Eddies and dipoles around South Madagascar: formation, pathways and large-scale impact. *Deep Sea Res. Part Oceanogr. Res. Pap.* 51: 383–400. <https://doi.org/10.1016/j.dsr.2003.10.011>
- Dong, H-P., Wang, D-Z., Dai, M., Hong, H-S., 2010. Characterization of particulate organic matters in the water column of the South China Sea using a shotgun proteomic approach. *Limnol. Oceanogr.* 55(4): 1565-1578. DOI: 10.4319/lo.2010.55.4.1565
- Dower, J., Freeland, H., Juniper, K., 1992. A strong biological response to oceanic flow past Cobb Seamount. *Deep Sea Res. Part Oceanogr. Res. Pap.* 39: 1139–1145. [https://doi.org/10.1016/0198-0149\(92\)90061-W](https://doi.org/10.1016/0198-0149(92)90061-W)
- Dubroca, L., Chassot, E., Floch, L., Demarcq, H., Assan, C., Delgado de Molina, A., 2013. Seamounts and tuna fisheries: Tuna hotspots or fishermen habits? *Collect. Vol. Sci. Pap. ICCAT*. 69(5): 2087-2102.
- Duffy, L.M., Kuhnert, P.M., Pethybridge, H.R., Young, J.W., Olson, R.J., Logan, J.M., Goñi, N., Romanov, E., Allain, V., Staudinger, M.D., Abecassis, M., Choy, C.A., Hobday, A.J., Simier, M., Galván-Magaña, F., Potier, M., Ménard, F., 2017. Global trophic ecology of yellowfin, bigeye, and albacore tunas: Understanding predation on micronekton communities at ocean-basin scales. *Deep-Sea Res. II*. 40: 55-73.

- <http://dx.doi.org/10.1016/j.dsr2.2017.03.003>
- Fabiano, M., Povero, P., Danovaro, R., 1993. Distribution and composition of particulate organic matter in the Ross Sea (Antarctica). *Polar Biol.* 13: 525-533.
- Fanelli, E., Cartes, J.E., Rumolo, P., Sprovieri, M., 2009. Food-web structure and trophodynamics of mesopelagic-suprabenthic bathyal macrofauna of the Algerian Basin based on stable isotopes of carbon and nitrogen. *Deep-Sea Res. I.* 56: 1504-1520.
DOI: 10.1016/j.dsr.2009.04.004
- Fanelli, E., Papiol, V., Cartes, J.E., Rumolo, P., Brunet, C., Sprovieri, M., 2011a. Food web structure of the epibenthic and infaunal invertebrates on the Catalan slope (NW Mediterranean): Evidence from $\delta^{13}\text{C}$ and $\delta^{15}\text{N}$ analysis. *Deep-Sea Res. I: Oceanographic Research Papers.* 58: 98-109.
<https://doi.org/10.1016/j.dsr.2010.12.005>
- Fanelli, E., Cartes, J.E., Papiol, V., 2011b. Food web structure of deep-sea macrozooplankton and micronekton off the Catalan slope: Insight from stable isotopes. *Journal of Marine Systems.* 87: 79-89. DOI: 10.1016/j.jmarsys.2011.03.003
- Fanelli, E., Papiol, V., Cartes, J.E., Rumolo, P., López-Pérez, C., 2013. Trophic webs of deep-sea megafauna on mainland and insular slopes of the NW Mediterranean: a comparison by stable isotope analysis. *Mar. Ecol. Prog. Ser.* 490: 199-221.
DOI: 10.3354/meps10430
- Feunteun, E., Miller, M.J., Carpentier, A., Aoyama, J., Dupuy, C., Kuroki, M., Pagano, M., Réveillac, E., Sellos, D., Watanabe, S., Tsukamoto, K., Otake, T., 2015. Stable isotopic composition of anguiliform leptocephali and other food web components from west of the Mascarene Plateau. *Prog. Oceanogr.* 137: 69-83.
<http://dx.doi.org/10.1016/j.pocean.2015.05.024>
- Fonteneau, A., 1991. Monts sous-marins et thons dans l'Atlantique tropical est. *Aquat. Living. Resour.* 4: 13-25.
- Foxton, P., Roe, H.S.J., 1974. Observations on the Nocturnal Feeding of some Mesopelagic Decapod Crustacea. *Mar. Biol.* 28: 37-49.
- France, R., Chandler, M., Peters, R., 1998. Mapping trophic continua of benthic foodwebs: body size- $\delta^{15}\text{N}$ relationships. *Mar. Ecol. Prog. Ser.* 174: 301-306.
- Fry, B., 1996. $^{13}\text{C}/^{12}\text{C}$ fractionation by marine diatoms. *Mar. Ecol. Prog. Ser.* 134: 283-294.
- Fry, B., 2006. *Stable Isotope Ecology*. Springer, New York. 308pp.
- Genin, A., Boehlert, G.W., 1985. Dynamics of temperature and chlorophyll structures above a seamount: An oceanic experiment. *J. Mar. Res.* 43: 907-924.
<https://doi.org/10.1357/002224085788453868>
- Go, Y.B., 1986. Diet and feeding chronology of mesopelagic micronektonic fish, *Diaphus suborbitalis*, in Suruga Bay, Japan. In: 1. Asian Fisheries Forum, Manila (Philippines), 26-31 May 1986.
- Guinet, C., Cherel, Y., Ridoux, V., Jouventin, P., 1996. Consumption of marine resources by seabirds and seals in Crozet and Kerguelen waters: changes in relation to consumer biomass 1962-85. *Antarctic Science.* 8(1): 23-30
- Halo, I., Backeberg, B., Penven, P., Ansoerge, I., Reason, C., Ullgren, J.E., 2014. Eddy properties in the Mozambique Channel: A comparison between observations and two numerical ocean circulation models. *Deep Sea Res. Part II Top. Stud. Oceanogr.* 100: 38-53. <http://dx.doi.org/10.1016/j.dsr2.2013.10.015>
- Harbou, L.V., 2009. Trophodynamics of salps in the Atlantic Southern Ocean. PhD thesis, Universität Bremen, Germany.

- Heffernan, J.T., Hopkins, T.L., 1981. Vertical Distribution and Feeding of the Shrimp Genera *Gennadas* and *Bentheogennema* (Decapoda: Penaeida) in the Eastern Gulf of Mexico. *Journal of Crustacean Biology*. 1(4): 461-473.
- Hesslein, R.H., Hallard, K.A., Ramlal, P., 1993. Replacement of Sulfur, Carbon, and Nitrogen in Tissue of Growing Broad Whitefish (*Coregonus nasus*) in Response to a Change in Diet Traced by $\delta^{34}\text{S}$, $\delta^{13}\text{C}$, and $\delta^{15}\text{N}$. *Can. J. Fish. Aquat. Sci.* 50: 2071-2076.
- Hidaka, K., Kawaguchi, K., Murakami, M., Takahashi, M., 2001. Downward transport of organic carbon by diel migratory micronekton in the western equatorial Pacific: its quantitative and qualitative importance. *Deep-Sea Res. I.* 48: 1923-1939
- Hirsch, S., Christiansen, B., 2010. The trophic blockage hypothesis is not supported by the diets of fishes on Seine Seamount. *Marine Ecology*. 31: 107–120.
<https://doi.org/10.1111/j.1439-0485.2010.00366.x>
- Hobson, K.A., Piatt, J.F., Pitocchelli, J., 1994. Using stable isotopes to determine seabird trophic relationships. *Journal of Animal Ecology*. 63: 786-798.
- Holland, K.N., Kleiber, P., Kajiura, S.M., 1999. Different residence times of yellowfin tuna, *Thunnus albacares*, and bigeye tuna, *T. obesus*, found in mixed aggregations over a seamount. *Fish. Bull.* 97: 392–395.
- Hopkins, T.L., Flock, M.E., Gartner, J.V. Jr., Torres, J.J., 1994. Structure and trophic ecology of a low latitude midwater decapod and mysid assemblage. *Mar. Ecol. Prog. Ser.* 109: 143-156.
- Hudson, J.M., Steinberg, D.K., Sutton, T.T., Graves, J.E., Latour, R.J., 2014. Myctophid feeding ecology and carbon transport along the northern Mid-Atlantic Ridge. *Deep-Sea Res. I.* 93:104-116. <https://doi.org/10.1016/j.dsr.2014.07.002>
- Hussey, N.E., MacNeil, M.A., McMeans, B.C., Olin, J.A., Dudley, S.F.J., Cliff, G., Wintner, S.P., Fennessy, S.T., Fisk, A.T., 2014. Rescaling the trophic structure of marine food webs. *Ecology Letters*, 17: 239-250. DOI: 10.1111/ele.12226
- Ingle, B., Koslow, J.A., 2005. Deep-sea ecosystems of the Indian Ocean. *Indian Journal of Marine Sciences*. 34(1): 27-34.
- IOTC Catch and Effort database. 2018. Available at
https://www.iotc.org/data/datasets?__cf_chl_jschl_tk__=ebffbdbd808fe0fa2e0ce342d88a0e0fa97fc63c-1578403316-0-AbYRwW88C8MO-1LnSVqSvpMqY3x_PGoxouNKuvGZy2X8De9NCy6mFx07f7GFtJjokedKCvEkJ5b7BwcYQtIX-A4KidGt1a6J9aAY9H8Y2ormKM543ixwdYh8d0HrniHi9P31fM1U8qyHBGexlhPFKYzXUxMKbV509-vD1mrSjYwW77ozbytXjlWcy3O2h_1C12C2-RJGWCsaxE2gxxw4xIWzXEFZ4tCh-YqOZRzXUpqxNgWBVaOxSTgNMboZj9PAKa1dIsFRs93SwtgNflbIgQg
- Jackson, A.L., Inger, R., Parnell, A.C., Bearhop, S., 2011. Comparing isotopic niche widths among and within communities: SIBER – Stable Isotope Bayesian Ellipses in R. *Journal of Animal Ecology*. 80: 595-602. DOI: 10.1111/j.1365-2656.2011.01806.x
- Jaquemet, S., Ternon, J.F., Kaehler, S., Thiebot, J.B., Dyer, B., Bemanaja, E., Marteau, C., Le Corre, M., 2014. Contrasted structuring effects of mesoscale features on the seabird community in the Mozambique Channel. *Deep-Sea Res. II.* 100: 200-211.
<http://dx.doi.org/10.1016/j.dsr2.2013.10.027>
- Kolasinski, J., Rogers, K., Frouin, P., 2008. Effects of acidification on carbon and nitrogen stable isotopes of benthic macrofauna from a tropical coral reef. *Rapid Commun Mass Spectrom.* 22: 2955–2960. DOI: 10.1002/rcm.3694
- Kolasinski, J., Kaehler, S., Jaquemet, S., 2012. Distribution and sources of particulate organic matter in a mesoscale eddy dipole in the Mozambique Channel (south-western Indian

- Ocean): Insight from C and N stable isotopes. *J. Mar. Syst.* 96-97: 122-131.
<https://doi.org/10.1016/j.jmarsys.2012.02.015>
- Karakulak, F.S., Salman, A., Oray, I.K., 2009. Diet composition of bluefin tuna (*Thunnus thynnus* L. 1758) in the Eastern Mediterranean Sea, Turkey. *J. Appl. Ichthyol.* 25: 757-761. DOI: 10.1111/j.1439-0426.2009.01298.x
- Koslow, J.A., 1997. Seamounts and the Ecology of Deep-Sea Fisheries: The firm-bodied fishes that feed around seamounts are biologically distinct from their deepwater neighbors-and may be especially vulnerable to overfishing. *American Scientist.* 85(2): 168-176.
- Lack, M., Short, K., Willock, A., 2003. Managing risk and uncertainty in deep-sea fisheries: lessons from Orange Roughy. TRAFFIC Oceania and WWF Endangered Seas Programme.
- Layman, C.A., Arrington, D.A., Montaña, C.G., Post, D.M., 2007. Can stable isotope ratios provide for community-wide measures of trophic structure? *Ecology.* 88: 42-48.
- Lecomte-Finiger, R., Maunier, C., Khafif, M., 2004. Leptocephali, these unappreciated larvae. *Cybium.* 28(2): 83-95.
- Liénart, C., Savoye, N., Bozec, Y., Breton, E., Conan, P., David, V., Feunteun, E., Grangeré, K., Kerhervé, P., Lebreton, B., Lefebvre, S., L'Helguen, S., Mousseau, L., Raimbault, P., Richard, P., Riera, P., Sauriau, P.-G., Schaal, G., Aubert, F., Aubin, S., Bichon, S., Boinet, C., Bourasseau, L., Bréret, M., Caparros, J., Cariou, T., Charlier, K., Claquin, P., Cornille, V., Corre, A.-M., Costes, L., Crispi, O., Crouvoisier, M., Czamanski, M., Del Amo, Y., Derriennic, H., Dindinaud, F., Durozier, M., Hanquiez, V., Nowaczyk, A., Devesa, J., Ferreira, S., Fournier, M., Garcia, F., Garcia, N., Geslin, S., Grossteffan, E., Gueux, A., Guillaudeau, J., Guillou, G., Joly, O., Lachaussée, N., Lafont, M., Lamoureux, J., Lecuyer, E., Lehodey, J.-P., Lemeille, D., Leroux, C., Macé, E., Maria, E., Pineau, P., Petit, F., Pujon-Pay, M., Rimelin-Maury, P., Sultan, E., 2017. Dynamics of particulate organic matter composition in coastal systems: A spatio-temporal study at multi-systems scale. *Progress in Oceanography* 156: 221-239.
<https://doi.org/10.1016/j.pocean.2017.03.001>
- Longhurst, A., 1998. *Ecological Geography of the Sea.* Academic Press, San Diego. 398p.
- Longhurst, A., 2007. The Indian Ocean-Indian South Subtropical Gyre Province (ISSG). In: Academic Press (Ed.), *Ecological Geography of the Sea*, 2nd ed. Elsevier, USA, pp 285.
- Lorrain, A., Graham, B.S., Popp, B.N., Allain, V., Olson, R.J., Hunt, B.P.V., Potier, M., Fry, B., Galván-Magaña, F., Menkes, C.E.R., Kaehler, S., Ménard, F., 2015. Nitrogen isotopic baselines and implications for estimating foraging habitat and trophic position of yellowfin tuna in the Indian and Pacific Oceans. *Deep-Sea Res. II.* 113: 188-198.
<https://doi.org/10.1016/j.dsr2.2014.02.003>
- Marsac, F., Fonteneau, A., Michaud, P., 2014. Le « Coco de Mer », une montagne sous la mer. In: *L'or bleu des Seychelles: Histoire de la pêche industrielle au thon dans l'océan Indien.* IRD Editions. 151-163.
- Marsac, F., Annasawmy, P., Noyon, M., Demarcq, H., Soria, M., Rabearisoa, N., Bach, P., Cherel, Y., Grelet, J., Romanov, E., 2020. Seamount effect on circulation and distribution of ocean taxa at and near La Pérouse, a shallow seamount in the southwestern Indian Ocean. *Deep-Sea II.*
- Martínez del Rio, C., Wolf, N., Carleton, S.A., Gannes, L.Z., 2009. Isotopic ecology ten years after a call for more laboratory experiments. *Biol. Rev.* 84: 91-111.
 DOI: 10.1111/j.1469-185X.2008.00064.x

- Mauchline, J., The Biology of the Euphausiid Crustacean, *Meganyctiphanes norvegica* (M. Sars). Proceedings of the Royal Society of Edinburgh, Section B: Biological Sciences. 67(2): 141-179
- Ménard, F., Benivary, H.D., Bodin, N., Coffineau, N., Le Loc'h, F., Mison, T., Richard, P., Potier, M., 2014. Stable isotope patterns in micronekton from the Mozambique Channel. Deep-Sea Research Part II: Topical Studies in Oceanography 100, 153–163. <https://doi.org/10.1016/j.dsr2.2013.10.023>
- Michener, R.H., Kaufman, L., 2007. Stable isotope ratios as tracers in marine food webs: an update. R.H. Michener, K. Lajtha (Eds.), Stable Isotopes in Ecology and Environmental Science (2nd ed.), Blackwell, Malden, MA (2007). pp. 238-282.
- Mill, A.C., Sweeting, C.J., Barnes, C., Al-Habsi, S.H., MacNeil, M.A., 2008. Mass-spectrometer bias in stable isotope ecology. Limnol. Oceanogr: Methods. 6(1): 34-39.
- Minagawa, M., Wada, E., 1984. Stepwise enrichment of ¹⁵N along food chains: further evidence and the relation between $\delta^{15}\text{N}$ and animal age. Geochim. Cosmochim. Acta. 48: 1135-1140.
- Mohn, C., White, M., 2007. Remote sensing and modelling of bio-physical distribution patterns at Porcupine and Rockall Bank, Northeast Atlantic. Cont. Shelf Res. 27: 1875-1892. DOI:10.1016/j.csr.2007.03.006
- Morato, T., Varkey, D.A., Damaso, C., Machete, M., Santos, M., Prieto, R., Santos, R.S., Pitcher, T.J., 2008. Evidence of a seamount effect on aggregating visitors. Mar. Ecol. Prog. Ser. 357: 23-32. DOI: 10.3354/meps07269
- Morato, T., Hoyle, S.D., Allain, V., Nicol, S.J., 2010. Tuna longline fishing around West and Central Pacific seamounts. PLoS ONE. 5(12): e14453. DOI: 10.1371/journal.pone.0014453
- Mouriño, B., Fernández, E., Serret, P., Harbour, D., Sinha, B., Pingree, R., 2001. Variability and seasonality of physical and biological fields at the Great Meteor Tablemount (subtropical NE Atlantic). Oceanol. Acta 24: 167–185. [https://doi.org/10.1016/S0399-1784\(00\)01138-5](https://doi.org/10.1016/S0399-1784(00)01138-5)
- Musyl, M.K., Brill, R.W., Boggs, C.H., Curran, D.S., Kazama, T.K., Seki, M.P., 2003. Vertical movements of bigeye tuna (*Thunnus obesus*) associated with islands, buoys, and seamounts near the main Hawaiian Islands from archival tagging data. Fish. Oceanogr. 12: 152–169. <https://doi.org/10.1046/j.1365-2419.2003.00229.x>
- Noyon, M., Morris, T., Walker, D., Huggett, J., 2018. Plankton distribution within a young cyclonic eddy off south-western Madagascar. Deep Sea Res. Part II Top. Stud. Oceanogr. In Press. <https://doi.org/10.1016/j.dsr2.2018.11.001>
- Noyon, M., Rasoloarijao, Z.T., Huggett, J., Roberts, M., Ternon, J-F., 2020. Comparison of mesozooplankton communities at three shallow seamounts in the South Western Indian Ocean using size spectrum analysis. Deep-Sea Res. II.
- Olivar, M.P., Bode, A., López-Pérez, C., Hulley, P.A., Hernández-León, S., 2019. Trophic position of lanternfishes (Pisces: Myctophidae) of the tropical and equatorial Atlantic estimated using stable isotopes. ICES Journal of Marine Science. DOI: 10.1093/icesjms/fsx243.
- Otake, T., Nogami, K., Maruyama, K., 1993. Dissolved and particulate organic matter as possible food sources for eel leptocephali. Mar. Ecol. Prog. Ser. 92: 27-34.
- Pakhomov, E. A., Perissinotto, R., & McQuaid, C. D., 1996. Prey composition and daily rations of myctophid fishes in the Southern Ocean. Mar. Ecol. Prog. Ser. 134, 1-14.
- Pakhomov, E.A., Henschke, N., Hunt, B.P.V., Stowasser, G., Cherel, Y., 2019. Utility of salps as a baseline proxy for food web studies. J. Plankton Res. 1-9.

DOI: 10.1093/plankt/fby051

- Papiol, V., Cartes, J.E., Fanelli, E., Rumolo, P., 2013. Food web structure and seasonality of slope megafauna in the NW Mediterranean elucidated by stable isotopes: Relationship with available food sources. *Journal of Sea Research*, 77: 53-69.
<http://dx.doi.org/10.1016/j.seares.2012.10.002>
- Parry, M., 2008. Trophic variation with length in two ommastrephid squids, *Ommastrephes bartramii* and *Sthenoteuthis oualaniensis*. *Mar. Biol.* 153: 249-256.
DOI: 10.1007/s00227-007-0800-3
- Paya, I., Montecinos, M., Ojeda, V., Cid, L., 2006. An overview of the orange roughy (*Hoplostethus* sp.) fishery off Chile. In: Shotton, R. (Ed.) *Deep Sea 2003: Conference on the Governance and Management of Deep-sea fisheries. Part 2: Conference poster papers and workshop papers.* Queenstown, New Zealand, 1-5 December 2003 and Dunedin, New Zealand 27-29 November 2003. *FAO Fisheries Proceedings No. 3/2*, Rome, FAO. 487 pp.
- Pearcy, W.G., Krygier, E.E., Mesecar, R., Ramsey, F., 1977. Vertical distribution and migration of oceanic micronekton off Oregon. *Deep-Sea Res.* 24: 223-245.
- Polunin, N.V.C., Morales-Nin, B., Pawsey, W.E., Cartes, J.E., Pinnegar, J.K., Moranta, J., 2001. Feeding relationships in Mediterranean bathyal assemblages elucidated by stable nitrogen and carbon isotope data. *Mar. Ecol. Prog. Ser.* 220: 13-23.
- Pomeroy, L.R., 2001. Caught in the food web: complexity made simple? *Sci. Mar.* 65 (Suppl. 2): 31-40.
- Portail, M., Olu, K., Dubois, S.F., Escobar-Briones, E., Gelinas, Y., Menot, L., Sarrazin, J., 2016. Food-Web Complexity in Guaymas Basin Hydrothermal Vents and Cold Seeps. *PLoS ONE*. 11(9): e0162263. DOI: 10.1371/journal.pone.0162263
- Post, D.M., Pace, M.L., Hairston, N.G.J., 2000. Ecosystem size determines food chain length in lakes. *Nature*. 405: 1047-1049.
- Post, D.M., 2002. Using stable isotopes to estimate trophic position: models, methods, and assumptions. *Ecology*. 83(3): 703-718.
- Potier, M., Marsac, F., Cherel, Y., Lucas, V., Sabatié, R., Maury, O., Ménard, F., 2007. Forage fauna in the diet of three large pelagic fishes (lancetfish, swordfish and yellowfin tuna) in the western equatorial Indian Ocean. *Fisheries Res.* 83: 60-72.
DOI: 10.1016/j.fishres.2006.08.020
- Preciado, I., Cartes, J.E., Punzón, A., Frutos, I., López-López, L., Serrano, A., 2017. Food web functioning of the benthopelagic community in a deep-sea seamount based on diet and stable isotope analyses. *Deep-Sea Res. II*: 137: 56-68.
<https://doi.org/10.1016/j.dsr2.2016.07.013>
- Quartly, G.D., Buck, J.J.H., Srokosz, M.A., Coward, A.C., 2006. Eddies around Madagascar-The retroflection re-considered. *J. Mar. Sci.* 63: 115-129.
DOI:10.1016/j.jmarsys.2006.06.001
- Ramanantsoa, J. D., Krug, M., Penven, P., Rouault, M., Gula, J., 2018. Coastal upwelling south of Madagascar: Temporal and spatial variability. *Journal of Marine Systems*, 178: 29-37. <https://doi.org/10.1016/j.jmarsys.2017.10.005>
- Reygondeau, G., Longhurst, A., Martinez, E., Beaugrand, G., Antoine, D., and Maury, O., 2013. Dynamic biogeochemical provinces in the global ocean. *Global Biogeochemical Cycles*, 27(4): 1046-1058. <http://doi.org/10.1002/gbc.20089>
- Riley, G.A., 1971. Particulate organic matter in sea water. *Advances in Marine Biology*. 8: 1-118. [https://doi.org/10.1016/S0065-2881\(08\)60491-5](https://doi.org/10.1016/S0065-2881(08)60491-5)
- Robison, B.H., 1984. Herbivory by the myctophid fish *Ceratoscopelus warmingii*. *Mar. Biol.* 84: 119-123.

- Rogers, A.D., 1994. The biology of seamounts. In *Advances in marine biology*. Academic Press. 30: 305-350.
- Romanov, E.V., 2003. Summary and review of Soviet and Ukrainian scientific and commercial fishing operations on the deep-water ridges of the southern Indian Ocean. (E. V Romanov, Ed.), *FAO Fisheries Circular C991*. Rome: FAO. <http://www.fao.org/DOCREP/006/Y4884E/Y4884E00.HTM>
- Romero-Romero, S., Choy, C.A., Hannides, C.C.S., Popp, B.N., Drazen, J.C., 2019. Differences in the trophic ecology of micronekton driven by diel vertical migration. *Limnol. Oceanogr.* 1-11. DOI: 10.1002/lno.11128
- Rubenstein, D.R., Hobson, K.A., 2004. From birds to butterflies: animal movement patterns and stable isotopes. *Trends in Ecology and Evolution*. 19(5): 256-263.
- Ryan, C., McHugh, B., Trueman, C.N., Harrod, C., Berrow, S., O'Connor, I., 2012. Accounting for the effects of lipids in stable isotope ($\delta^{13}\text{C}$ and $\delta^{15}\text{N}$ values) analysis of skin and blubber of balaenopterid whales. *Rapid Commun. Mass Spectrom.* 26: 2745-2754. DOI: 10.1002/rcm.6394
- Saino, T., Hattori, A., 1987. Geographical variation of the water column distribution of suspended particulate organic nitrogen and its ^{15}N natural abundance in the Pacific and its marginal seas. *Deep-Sea Res.* 34(5/6): 807-827.
- Savoie, N., Aminot, A., Tréguer, P., Fontugne, M., Naudet, N., Kérouel, R., 2003. Dynamics of particulate organic matter $\delta^{15}\text{N}$ and $\delta^{13}\text{C}$ during spring phytoplankton blooms in a macrotidal ecosystem (Bay of Seine, France). *Mar. Ecol. Prog. Ser.* 255: 27-41.
- Sholto-Douglas, A.D., Field, J.G., James, A.G., van der Merwe, N.J., 1991. $^{13}\text{C}/^{12}\text{C}$ and $^{15}\text{N}/^{14}\text{N}$ isotope ratios in the Southern Benguela Ecosystem: indicators of food web relationships among different size-classes of plankton and pelagic fish; differences between fish muscle and bone collagen tissues. *Mar. Ecol. Prog. Ser.* 78: 23-31.
- Smith, M.M., Heemstra, P.C., 1986. *Smith's Sea Fishes*. J.L.B. Smith Institute of Ichthyology, Grahamstown, South Africa. 1047 p.
- Sutton, T.T., 2013. Vertical ecology of the pelagic ocean: classical patterns and new perspectives. *J. Fish. Biol.* 83: 1508-1527. DOI: 10.1111/jfb.12263
- Tanaka, H., Ohshimo, S., Sassa, C., & Aoki, I., 2007. Feeding habits of mesopelagic fishes off the coast of western Kyushu, Japan. *PICES 16th: Bio*, p-4200. 1st November.
- Tew-Kai, E., Marsac, F., 2009. Patterns of variability of sea surface chlorophyll in the Mozambique Channel: a quantitative approach. *J. Mar. Syst.* 77 (1-2): 77-88. DOI: 10.1016/j.jmarsys.2008.11.007
- Utrecht, W.L., van Utrecht-Cock, C.N., De Graaf, A.M.J., 1987. Growth and seasonal variations in distribution of *Chauliodus sloani* and *C. danae* (pisces) from the mid north atlantic. *Bijdragen tot de Dierkunde*. 57(2): 164-182.
- Valls, M., Sweeting, C.J., Olivar, M.P., Fernández de Puellas, M.L., Pasqual, C., Polunin, N.V.C., Quetglas, A., 2014a. Structure and dynamics of food webs in the water column on shelf and slope grounds of the western Mediterranean. *Journal of Marine Systems*. 138: 171: 181. <http://dx.doi.org/10.1016/j.jmarsys.2014.04.002>
- Valls, M., Olivar, M.P., Fernández de Puellas, M.L., Molí, B., Bernal, A., Sweeting, C.J., 2014b. Trophic structure of mesopelagic fishes in the western Mediterranean based on stable isotopes of carbon and nitrogen. *Journal of Marine Systems*. 138: 160-170. <http://dx.doi.org/10.1016/j.jmarsys.2014.04.007>
- van der Spoel, S., Bleeker, J., 1991. Distribution of Myctophidae (Pisces, Myctophiformes) during the four seasons in the mid North Atlantic. *Contributions to Zoology*. 61(2): 89-106.
- Vanderklift, M.A., Ponsard, S., 2003. Sources of variation in consumer-diet $\delta^{15}\text{N}$ enrichment: a meta-analysis. *Oecologia*. 136(2): 169-182.

- Ventura, M., Catalan, J., 2008. Incorporating life histories and diet quality in stable isotope interpretations of crustacean zooplankton. *Freshwater Biology*. 53: 1453-1469.
DOI: 10.1111/j.1365-2427.2008.01976.x
- Vianello, P., Ternon, J-F., Herbette, S., Demarcq, H., Roberts, M.J., 2020. Circulation and hydrography in the vicinity of a shallow seamount on the northern Madagascar Ridge. *Deep-Sea Res. II*.
- Vipin, P.M., Harikrishnan, M., Renju, R., Boopendranath, M.R., Remesan, M.P., 2018. Population Dynamics of Spinycheek Lanternfish *Benthoosema fibulatum* (Gilbert and Cramer 1897), Caught off the South- west Coast of India. *Asian Fisheries Science*. 31: 161-171.
- Waite, A.M., Muhling, B.A., Holl, C.M., Beckley, L.E., Montoya, J.P., Strzelecki, J., Thompson, P.A., Pesant, S., 2007. Food web structure in two counter-rotating eddies based on $\delta^{15}\text{N}$ and $\delta^{13}\text{C}$ isotopic analyses. *Deep-Sea Res. II*. 54: 1055-1075.
DOI: 10.1016/j.dsr2.2006.12.010
- Watanuki, Y., Thiebot, J-B., 2018. Factors affecting the importance of myctophids in the diet of the world's seabirds. *Mar. Biol.* 165: 79. <https://doi.org/10.1007/s00227-018-3334-y>
- Young, J.W., Hunt, B.P.V., Cook, T.R., Llopiz, J.K., Hazen, E.L., Pethybridge, H.R., Ceccareli, D., Lorrain, A., Olson, R.J., Allain, V., Menkes, C., Patterson, T., Nicol, S., Lehodey, P., Kloser, R.J., Arrizabalaga, H., Choy, C.A., 2015. The trophodynamics of marine top predators: Current knowledge, recent advances and challenges. *Deep Sea-Res. II*. 113: 170-187. <http://dx.doi.org/10.1016/j.dsr2.2014.05.015>

List of tables and figures:

Table 1 Linear regression models fitted to $\delta^{15}\text{N}$ values (‰) with respect to body length in mm (SL, standard length for fish; TL, total length for leptocephali; ACL, abdomen and carapace length for the crustacean; DML, dorsal mantle length for the squid specimen) and the seamount variable (whether values were significantly different between La Pérouse and MAD-Ridge) of eight micronekton taxa- *Sigmops elongatus* (fish), *Ceratoscopelus warmingii* (fish), *Argyropelecus aculeatus* (fish), *Funchalia* sp. (crustacean), *Diaphus suborbitalis* (fish), *Abraliopsis* sp. (squid), *Chauliodus sloani* (fish), and leptocephali (fish).

Figure 1(a) Location of the MAD-Ridge and La Pérouse seamounts (black diamond symbols) in the East African Coastal (EAFR) and Indian South Subtropical Gyre (ISSG) provinces, respectively. Longhurst's (1998) biogeochemical provinces are delimited by black solid lines. Landmasses are shown in grey. Trawls #18-21 in the southern Mozambique Channel are shown by black stars and labelled "Trawl MZC". Map of (b) La Pérouse trawl stations numbered 1 to 10, (c) MAD-Ridge trawl stations numbered 1 to 17 plotted on the bathymetry (m). The colour bar indicates depth (m) below the sea surface.

Figure 2 Averaged satellite image of surface chlorophyll *a* concentrations from 18/09/2016 to 07/12/2016 at La Pérouse and MAD-Ridge (represented by black star symbols). The colour bar indicates the surface mean concentrations in mg m^{-3} . Monthly mean sea surface chlorophyll *a* concentrations (mg m^{-3}) from January to December 2016 for the regions defined by the red squares. The dates of the La Pérouse and MAD-Ridge cruises are marked by grey bars.

Figure 3. Bivariate plots of $\delta^{15}\text{N}$ and $\delta^{13}\text{C}$ values (‰) for particulate organic matter at the surface (POM-Surf) and the maximum fluorescence (POM-Fmax), zooplankton, gelatinous organisms, crustaceans, squid and mesopelagic fish sampled at La Pérouse and MAD-Ridge seamounts. Standard ellipse areas (coloured solid lines), calculated using SIBER, provide estimates of the size of the isotopic niche for each of these categories.

Figure 4. Boxplots of $\delta^{13}\text{C}$ and $\delta^{15}\text{N}$ values (‰) of the foodweb components POM-Surf, POM-Fmax, zooplankton (Zoopk), gelatinous organisms (Gel), crustaceans (Crust), squid and mesopelagic fish at La Pérouse (PER) and MAD-Ridge (MAD). Groups having significantly different $\delta^{13}\text{C}$ and $\delta^{15}\text{N}$ values (‰) are shown by solid blue lines.

Figure 5. $\delta^{15}\text{N}$ (mean \pm S.D.) values (‰) and estimated trophic level (TL estimated from the TPA method) of POM-Surf, POM-Fmax, zooplankton, gelatinous and sampled micronekton species at the La Pérouse and MAD-Ridge seamounts. Taxa are placed in broad categories and $\delta^{15}\text{N}$ compositions are sorted in ascending order of their values.

Figure 6. Hierarchical clustering (Euclidean distance of normalised data subjected to averaged grouping) of $\delta^{13}\text{C}$ and $\delta^{15}\text{N}$ values (‰) of sampled gelatinous organisms, crustaceans, squid and mesopelagic fish at La Pérouse and MAD-Ridge. Roman numerals at the tree branches identify groups of species belonging to the different trophic guilds: group I – filter-feeders and detritivores; group II- omnivores and carnivores; subgroup IA: filter-feeders at La Pérouse and MAD-Ridge; subgroup IB: detritivores at both seamounts; subgroup IIA: filter-feeders and omnivorous crustaceans at La Pérouse, highest trophic level mesopelagic fish at MAD-Ridge; subgroups IIB: omnivorous and carnivorous micronekton at La Pérouse and MAD-Ridge.

Figure 7. $\delta^{15}\text{N}$ values (‰) of (a) fish: *Sigmops elongatus*, (b) fish: *Ceratoscopelus warmingii*, (c) fish: *Argyropelecus aculeatus*, (d) crustacean: *Funchalia* sp., (e) fish: *Diaphus suborbitalis*, (f) squid: *Abraliopsis* sp., (g) fish: *Chauliodus sloani*, (h) fish: leptocephali, plotted against size in mm [standard length for (a)-(c), (e), (g)-(h); abdomen and carapace length for (d); dorsal mantle length for (f)] at La Pérouse (squares) and MAD-Ridge (stars). Simple linear regressions for $\delta^{15}\text{N}$ values versus size are plotted for (a)-(d).

Figure 8(a) $\delta^{15}\text{N}$ values (‰) of mesopelagic fish from La Pérouse and MAD-Ridge seamount vicinities (LP_Vicinity and MR_Vicinity respectively) and from the Mozambique Channel, plotted against their standard lengths (mm). Simple linear regressions are plotted. (b) Bivariate plots of $\delta^{15}\text{N}$ and $\delta^{13}\text{C}$ values (‰) for selected seamount flank- and summit-associated fish species *D. suborbitalis* at La Pérouse (LP) and *B. fibulatum*, *D. knappi*, *C. japonicus* and *D. suborbitalis* at MAD-Ridge (MR) seamounts. Standard lengths are given in mm.

Figure 9. Boxplots of $\delta^{13}\text{C}$ and $\delta^{15}\text{N}$ values (‰) of omnivorous/carnivorous mesopelagic fish at La Pérouse flank (n = 50 samples) and vicinity (n = 60 samples) stations and, MAD-Ridge vicinity (n = 91 samples), flank (n = 38 samples) and summit (n = 4 samples) stations, and stations from the southern Mozambique Channel (n = 28 samples). Outliers are shown as star symbols.

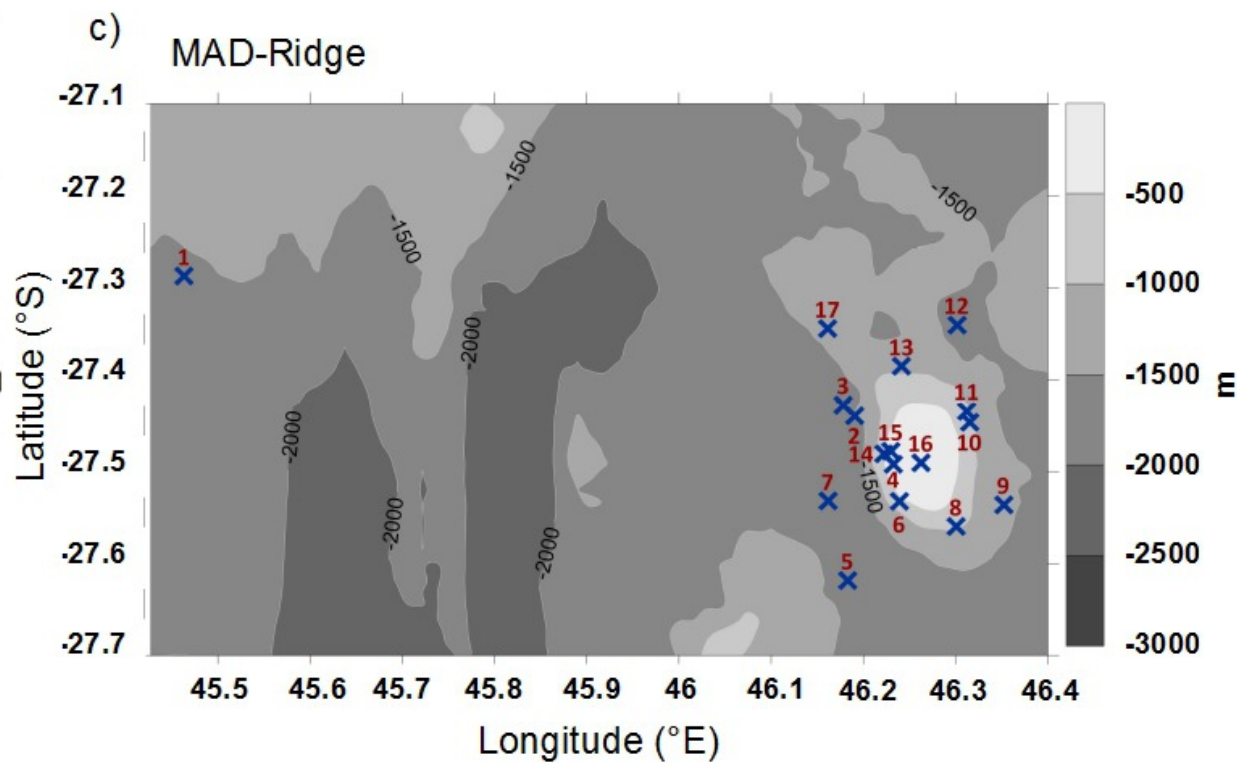
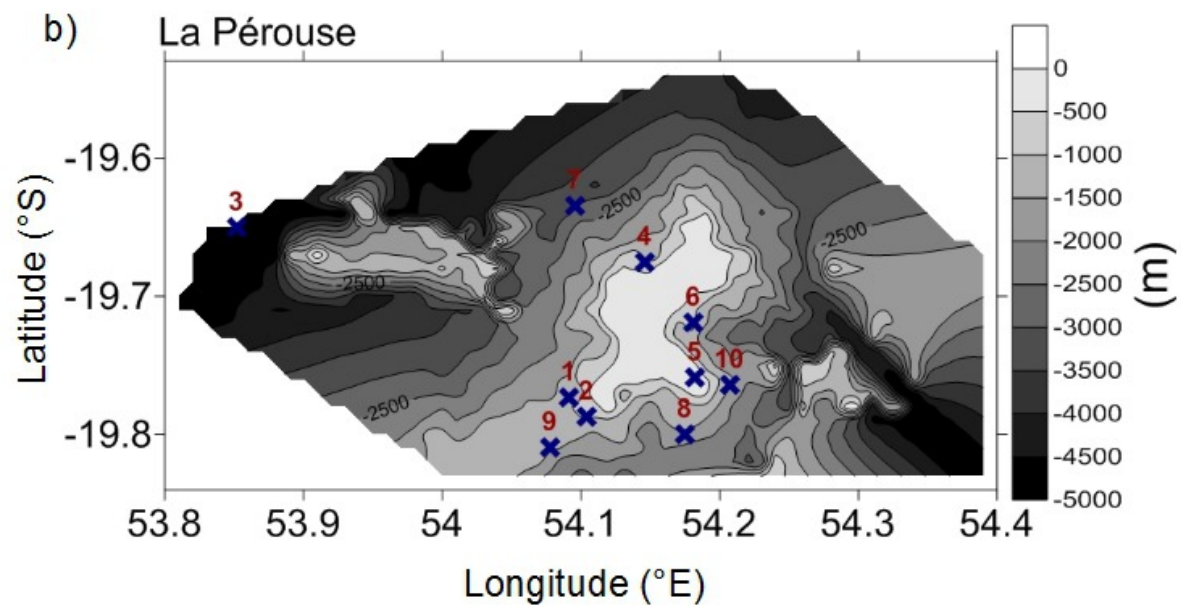
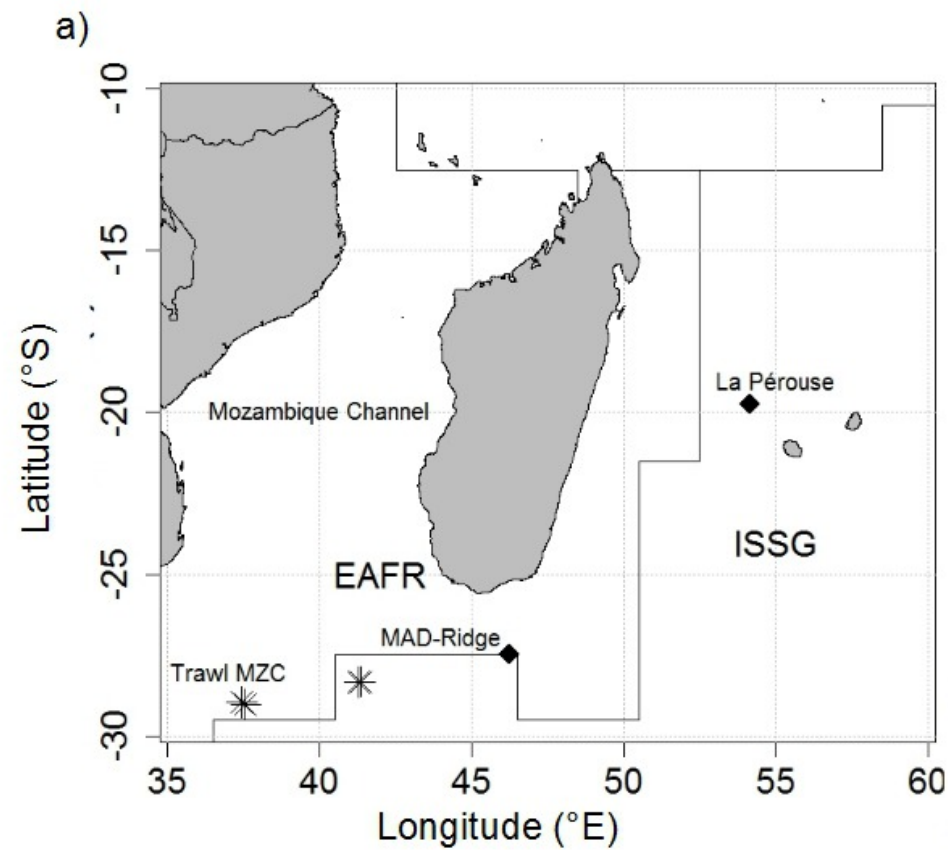


Figure 1

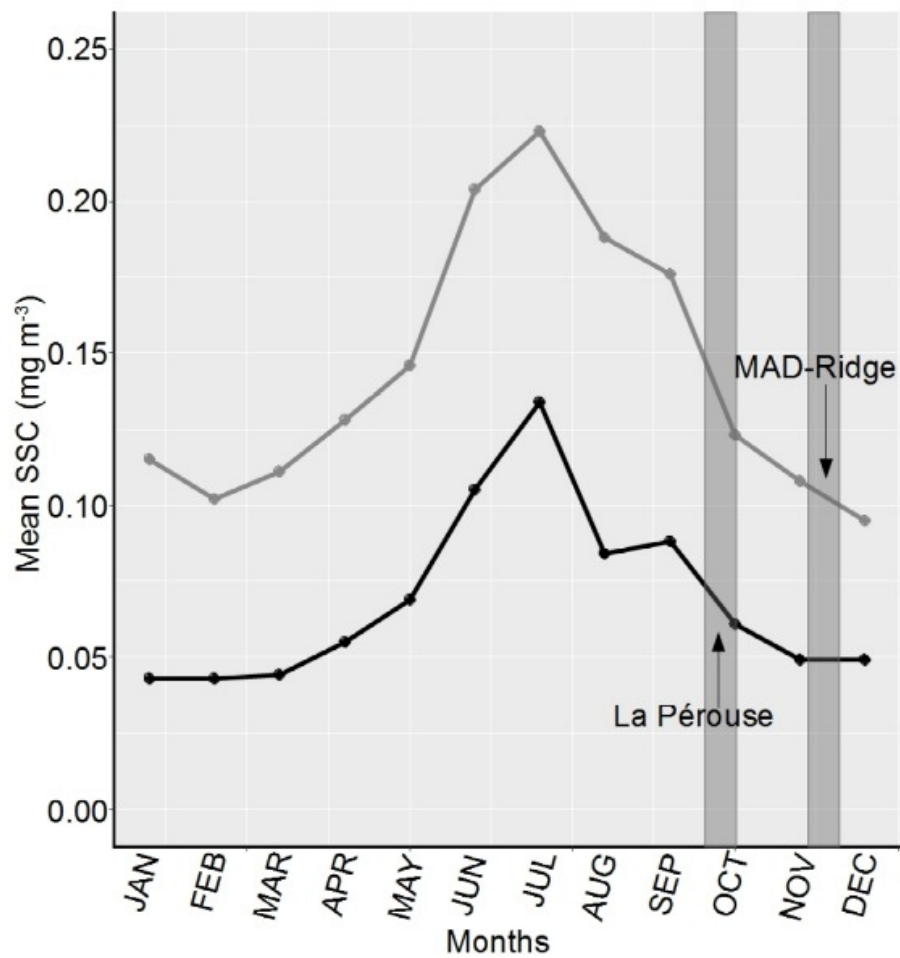
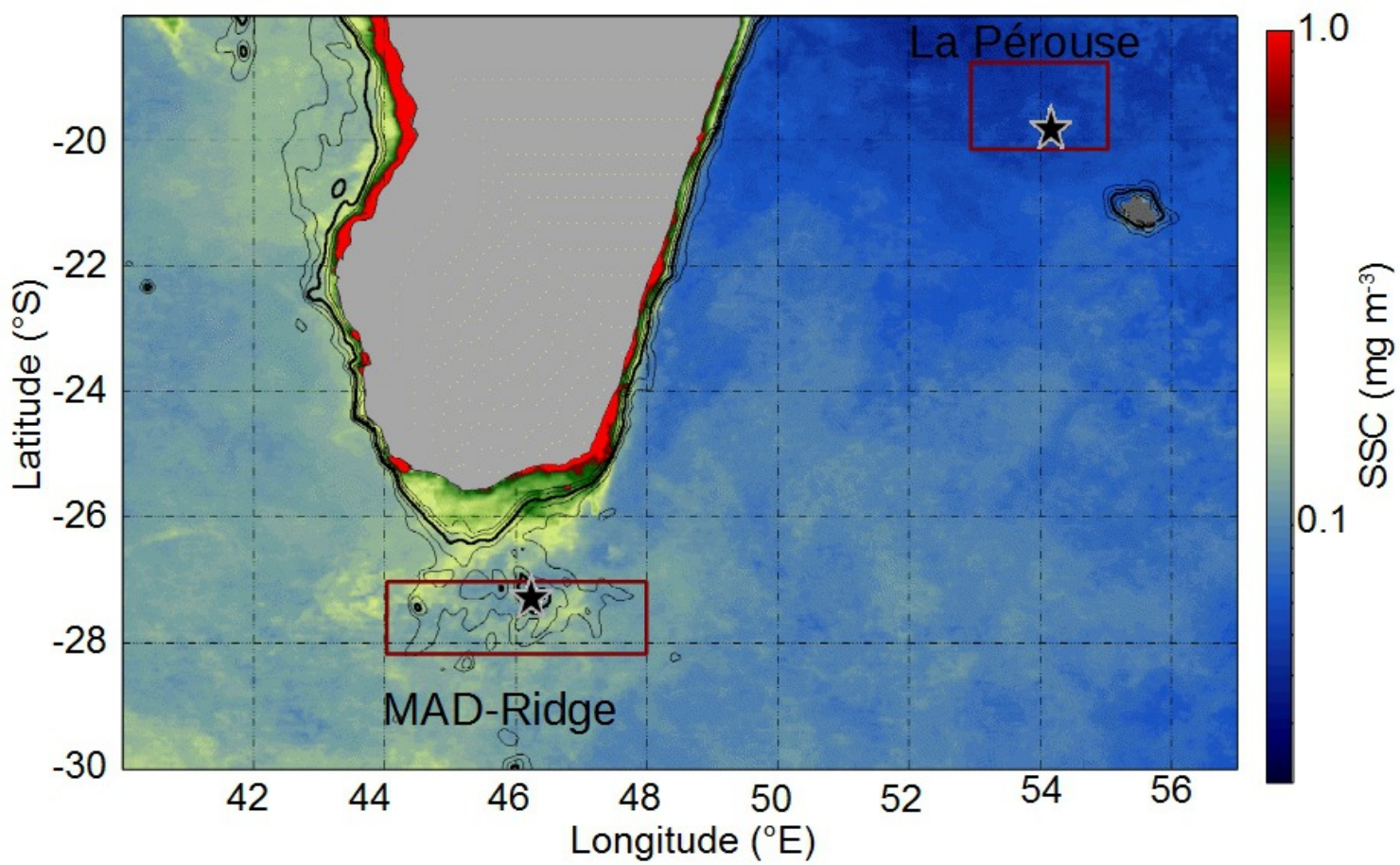
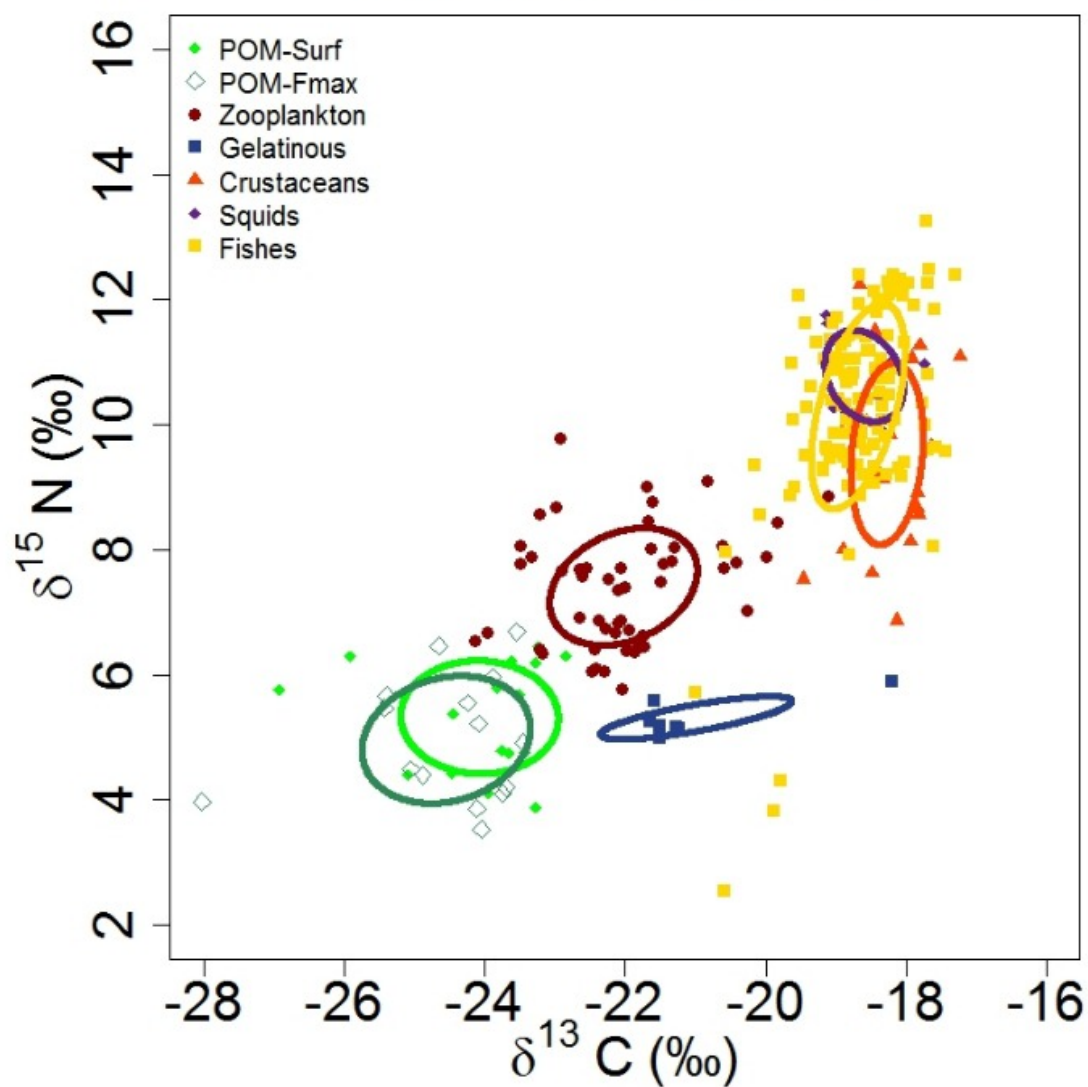


Figure 2

La Pérouse seamount



MAD-Ridge seamount

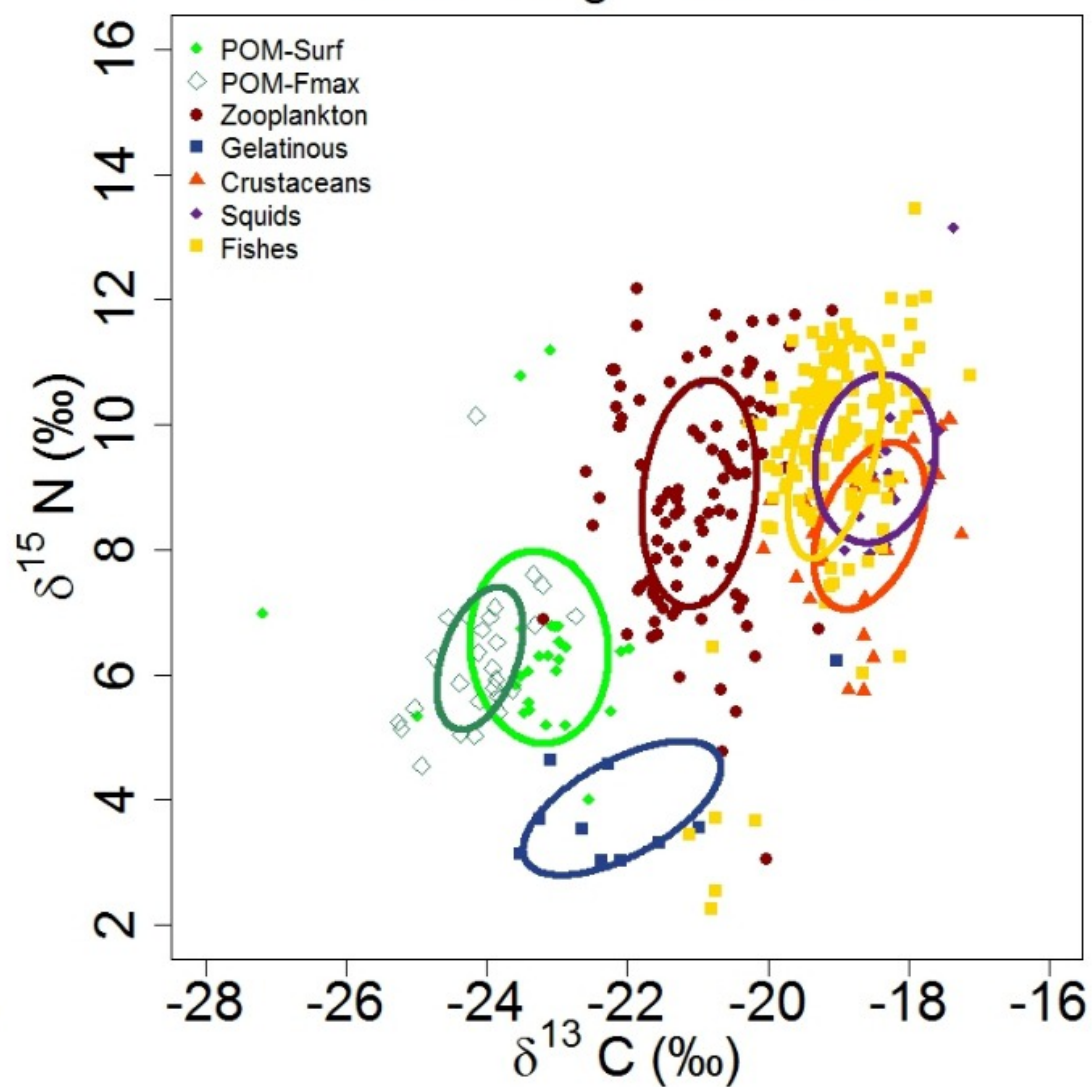


Figure 3

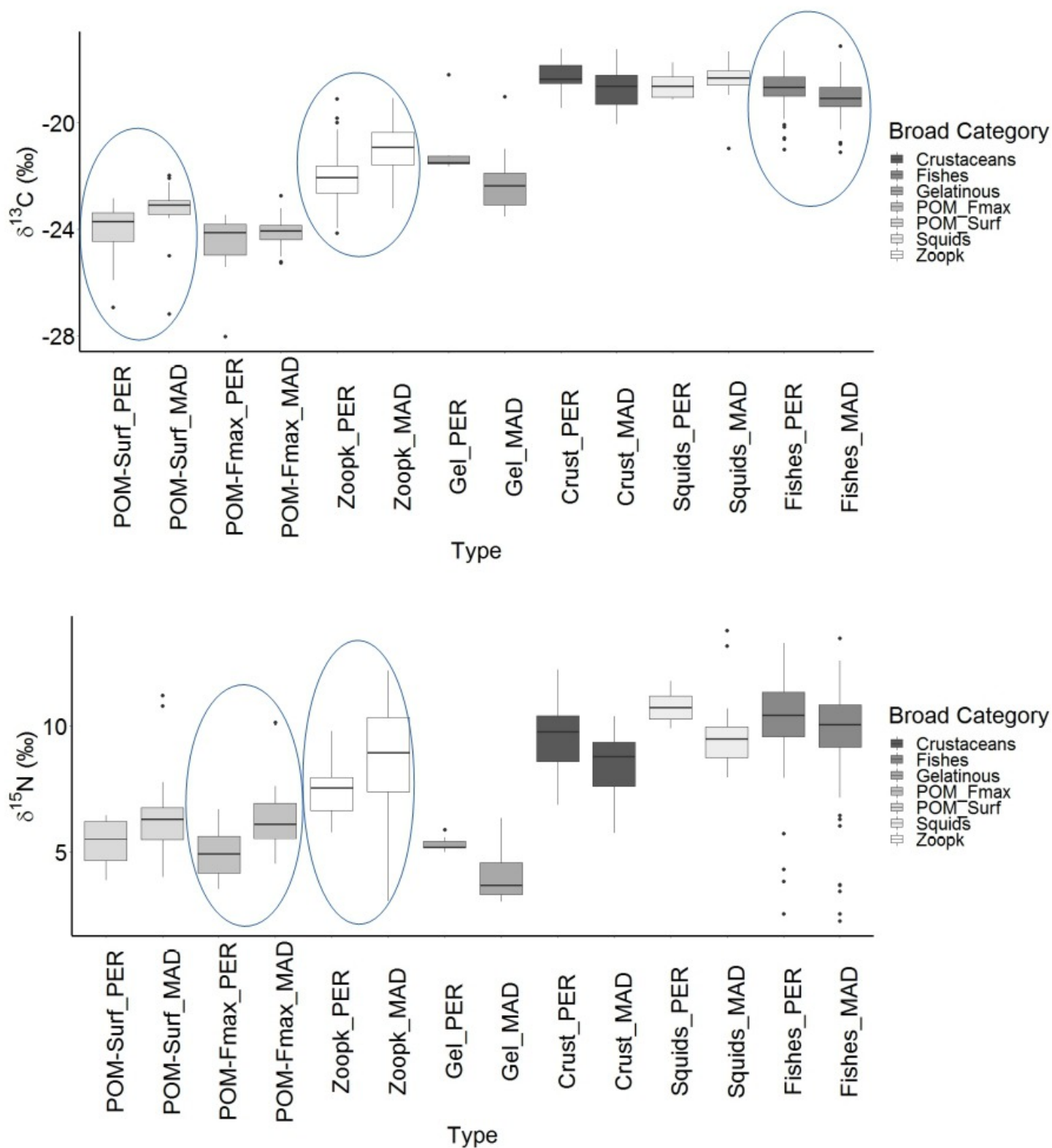


Figure 4

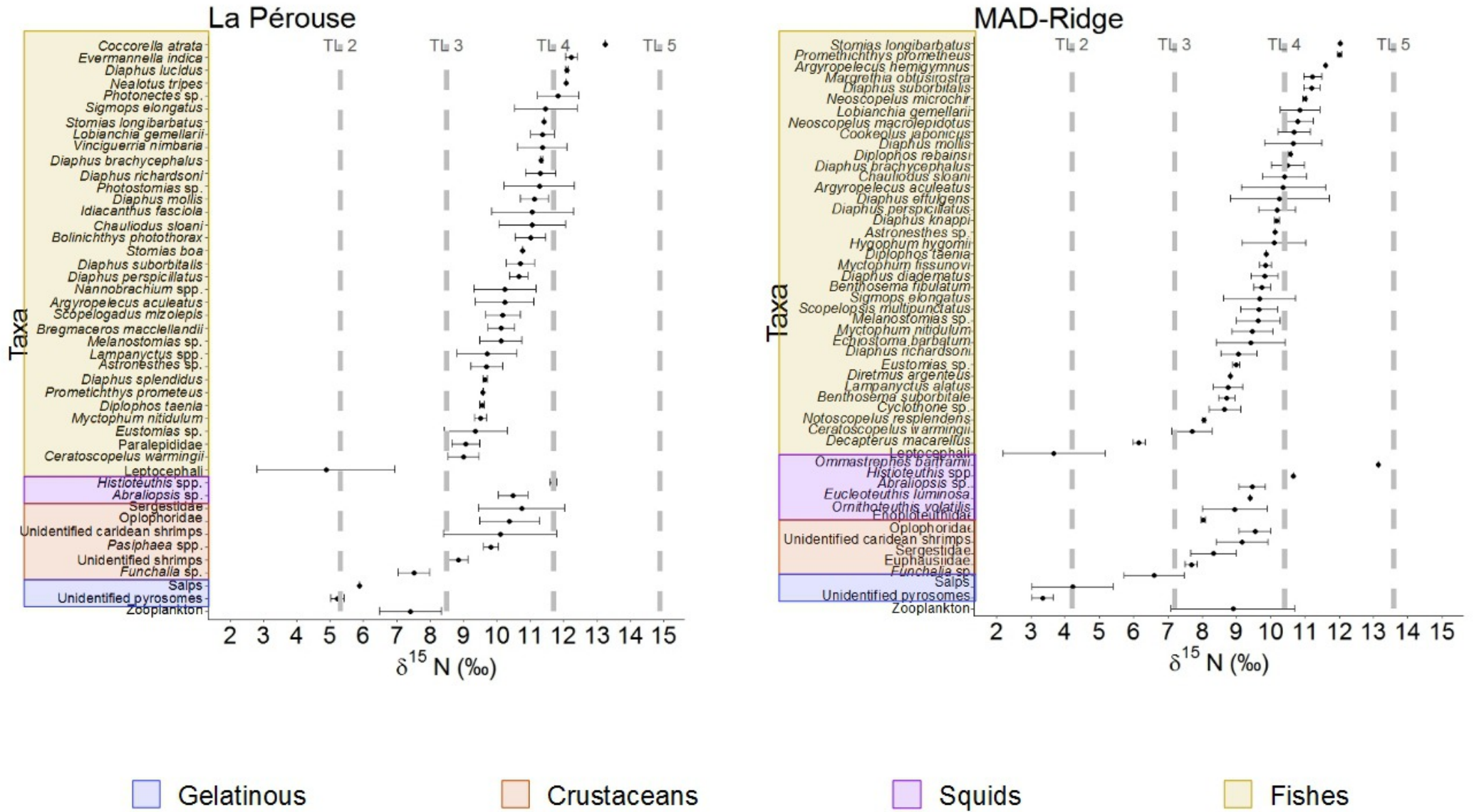


Figure 5

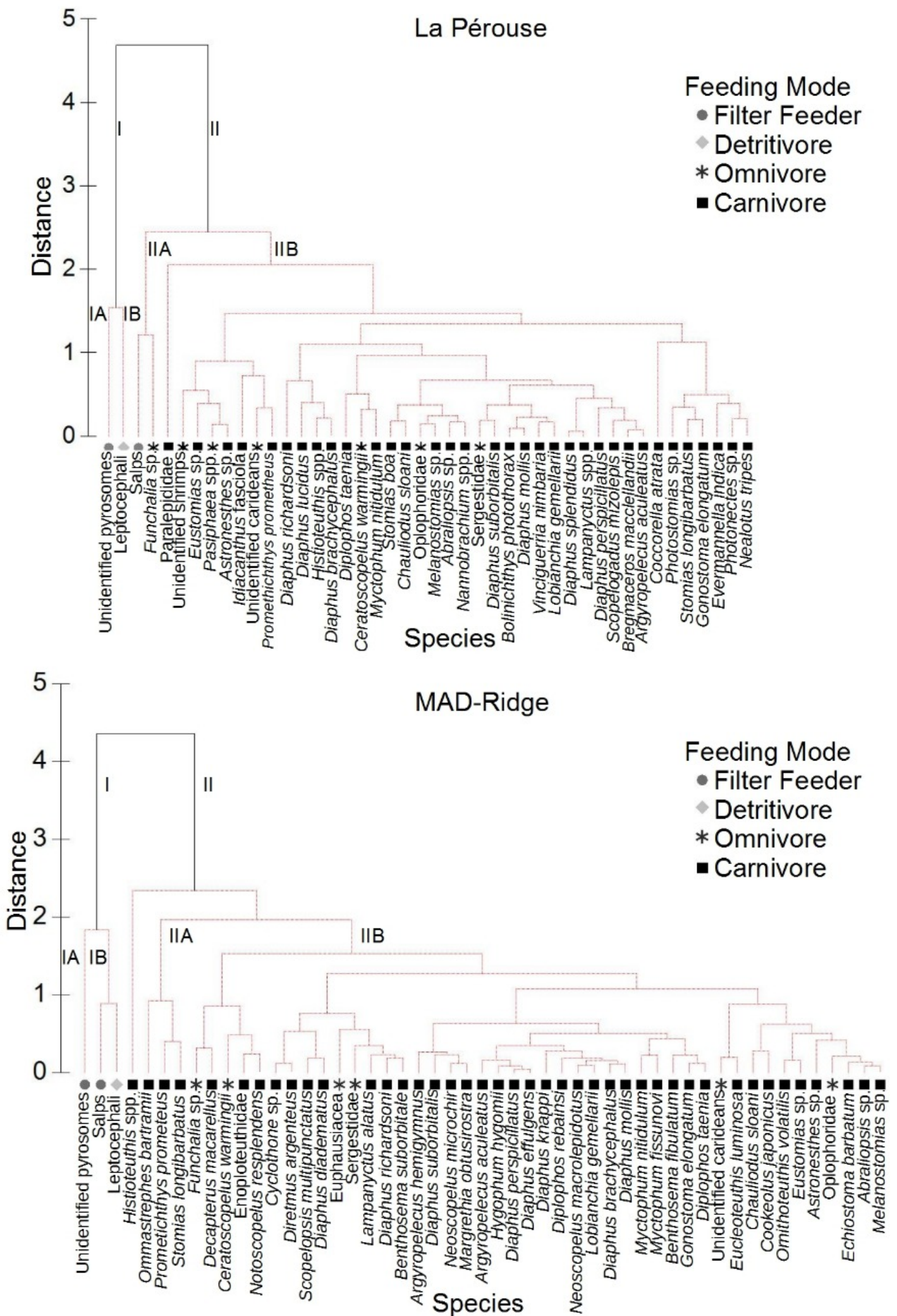


Figure 6

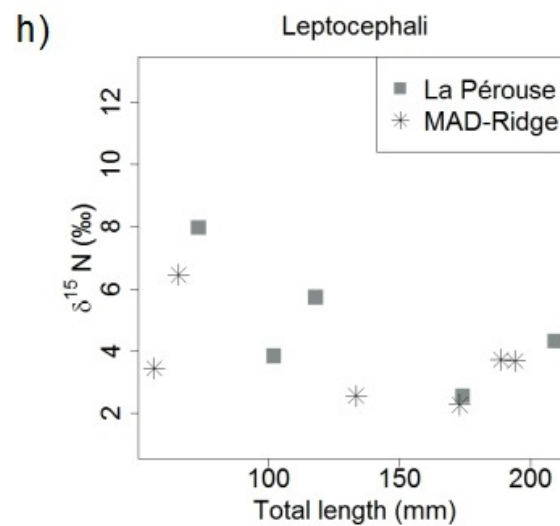
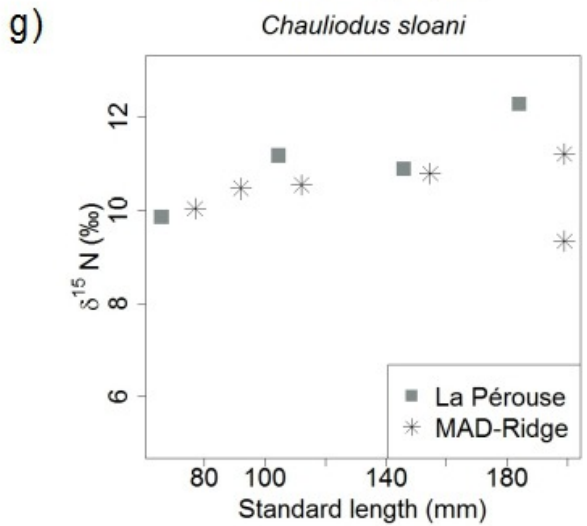
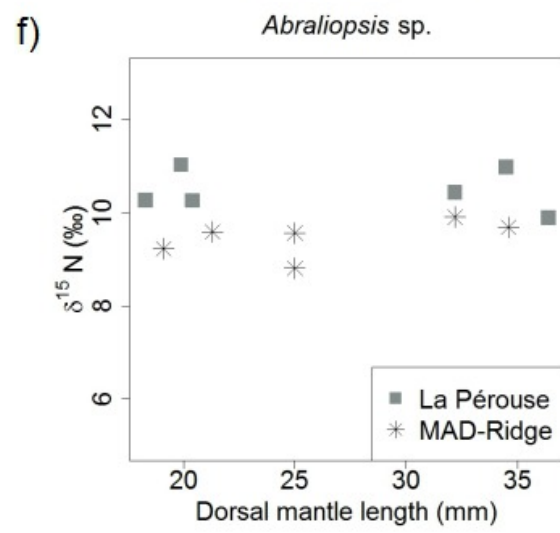
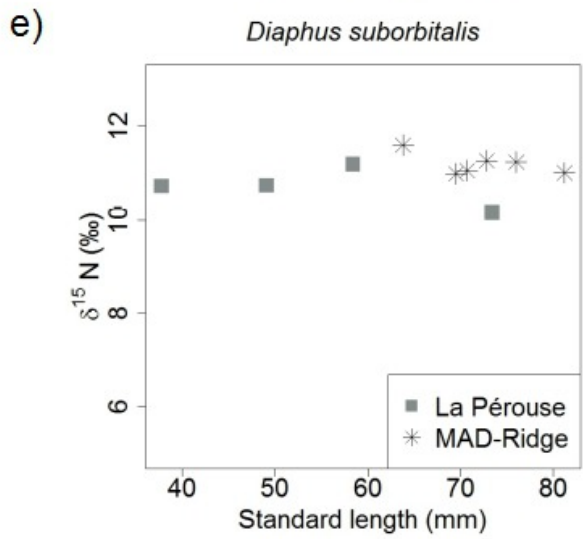
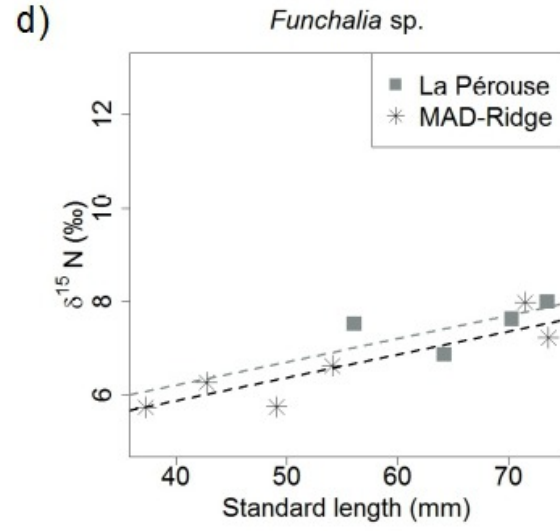
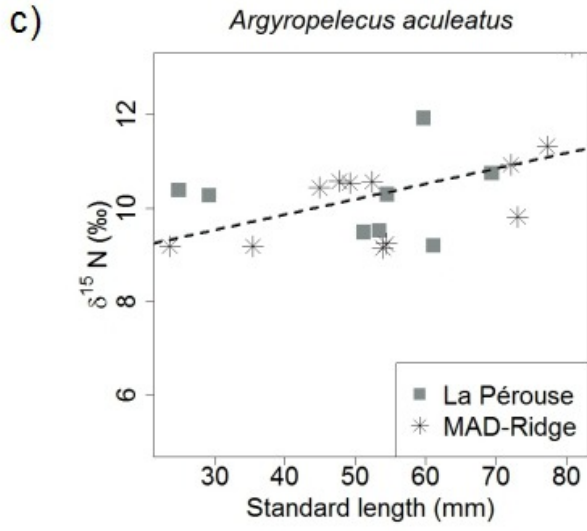
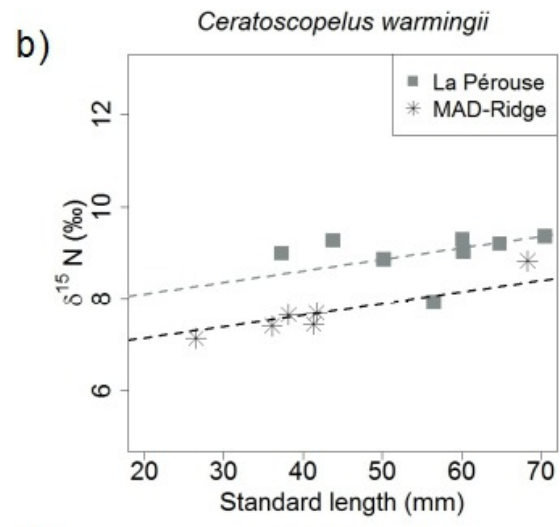
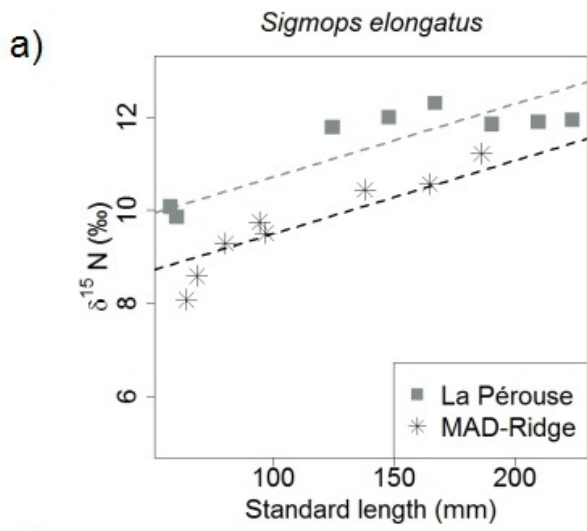
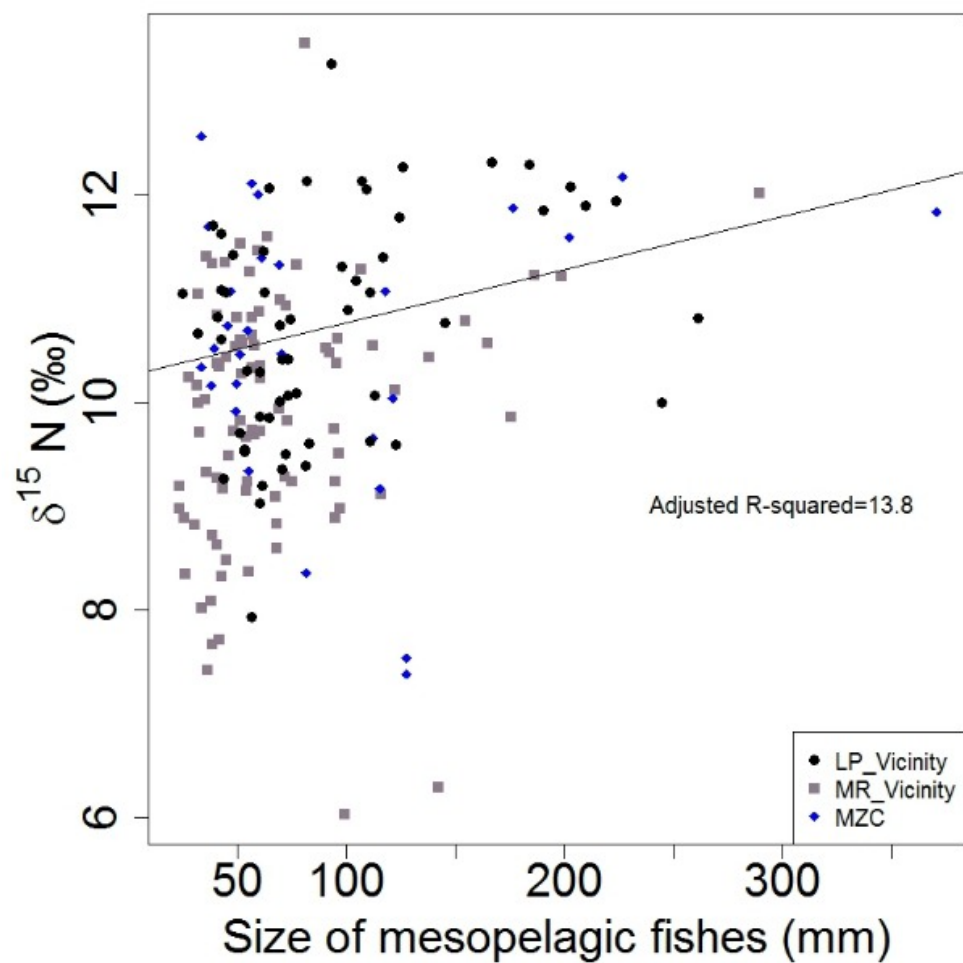


Figure 7

a)



b)

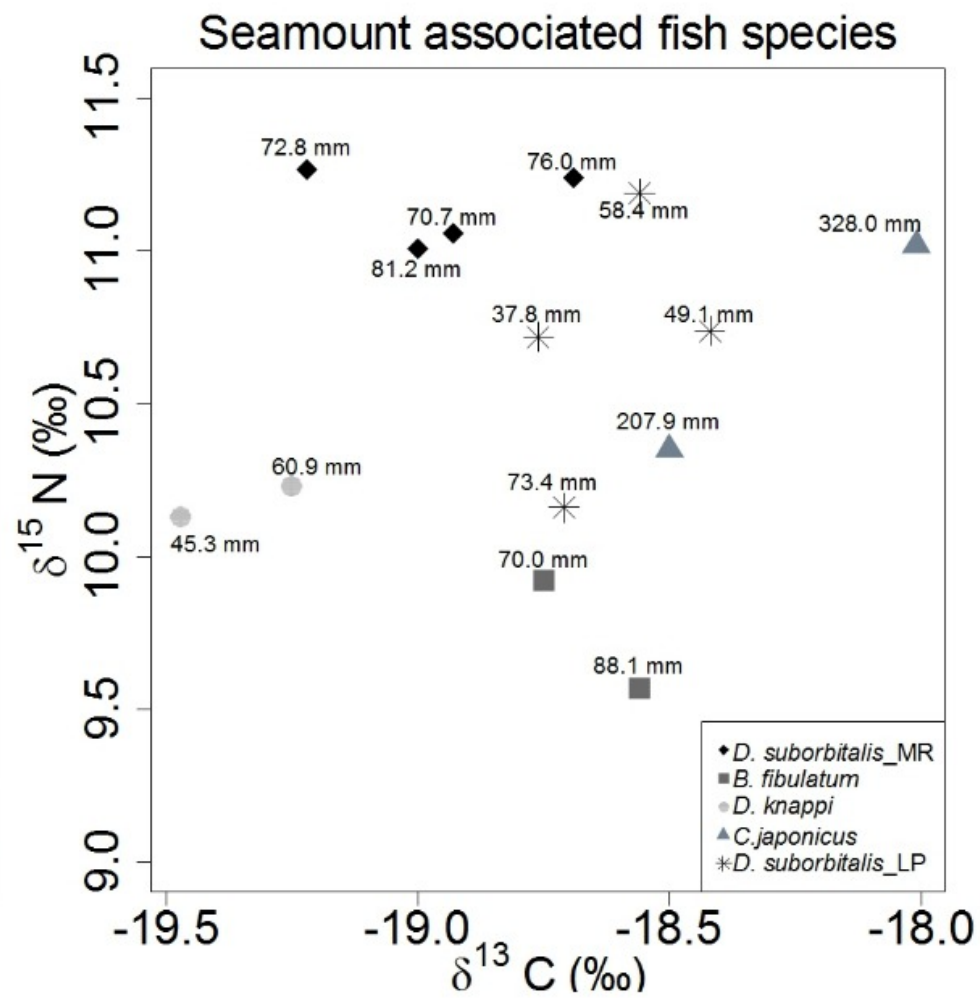


Figure 8

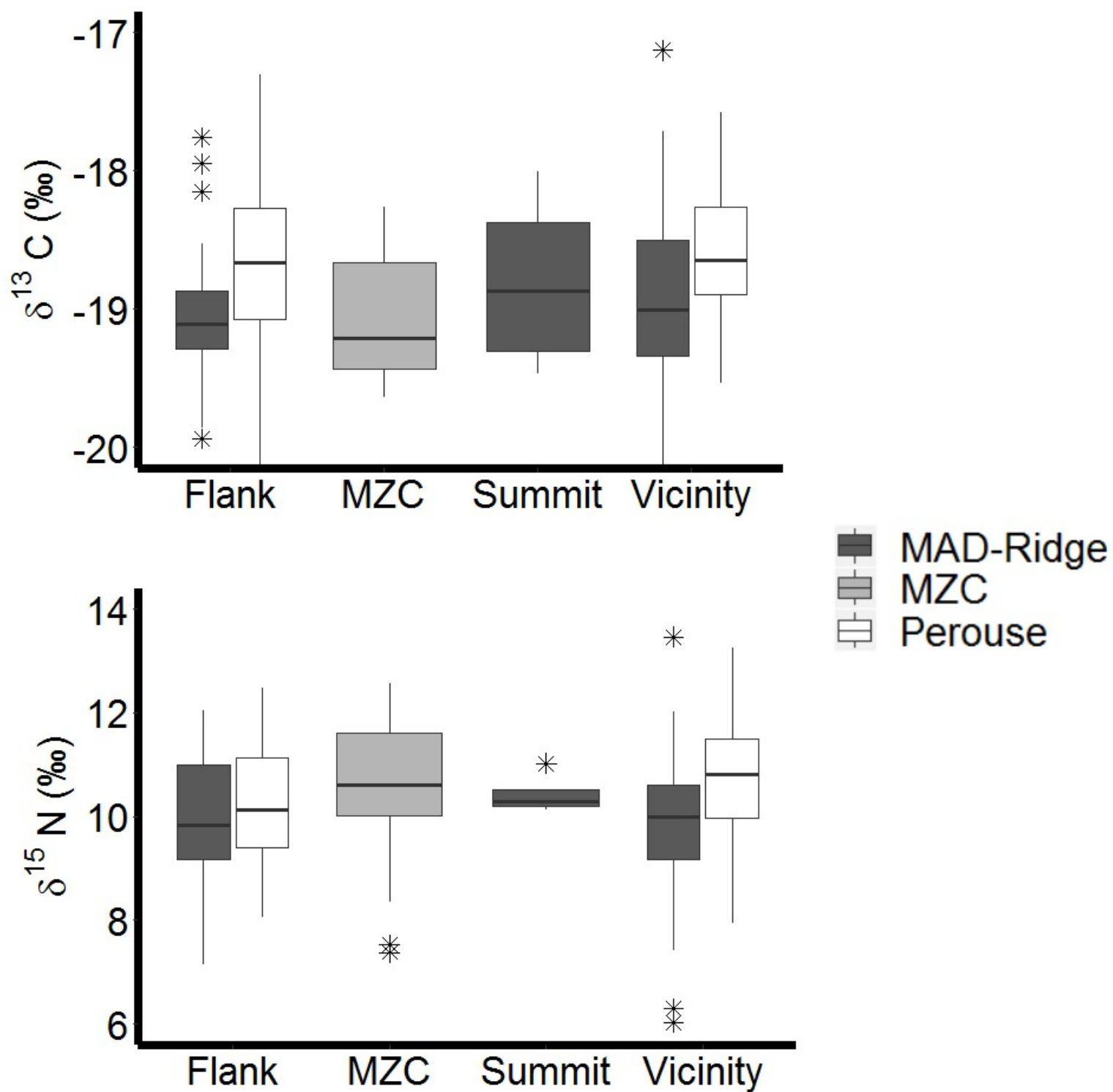


Figure 9

Table 1 Linear regression models fitted to $\delta^{15}\text{N}$ values (‰) with respect to body length in mm (SL, standard length for fishes; TL, total length for leptocephali larvae; ACL, abdomen and carapace length for the crustacean; DML, dorsal mantle length for the squid specimen) and the seamount variable (whether values were significantly different between La Pérouse and MAD-Ridge) of 8 micronekton taxa- *Sigmops elongatus* (fish), *Ceratoscopelus warmingii* (fish), *Argyropelecus aculeatus* (fish), *Funchalia* sp. (crustacean), *Diaphus suborbitalis* (fish), *Abraliopsis* sp. (squid), *Chauliodus sloani* (fish), and leptocephali (fish).

Taxon	Regression equation	Adjusted r^2 (%)	F-statistic	Degrees of freedom	P-value
<i>Sigmops elongatus</i>	$\delta^{15}\text{N} = 9.15 + 0.0157 \times \text{SL} - 1.2210 \times \text{seamount}$ La Pérouse: $\delta^{15}\text{N} = 9.15 + 0.0157 \times \text{SL}$ MAD-Ridge: $\delta^{15}\text{N} = 7.93 + 0.0157 \times \text{SL}$	85.2	46.0	13	< 0.05 for size and seamount
<i>Ceratoscopelus warmingii</i>	$\delta^{15}\text{N} = 7.61 + 0.0249 \times \text{SL} - 0.9521 \times \text{seamount}$ La Pérouse: $\delta^{15}\text{N} = 7.61 + 0.0249 \times \text{SL}$ MAD-Ridge: $\delta^{15}\text{N} = 6.66 + 0.0249 \times \text{SL}$	72.4	18.0	11	< 0.05 for size and seamount
<i>Argyropelecus aculeatus</i>	$\delta^{15}\text{N} = 8.57 + 0.0331 \times \text{SL} - 0.0272 \times \text{seamount}$	16.5	2.87	17	< 0.05 for size; > 0.05 for seamount
<i>Funchalia</i> sp.	$\delta^{15}\text{N} = 4.23 + 0.0496 \times \text{ACL} - 0.3460 \times \text{seamount}$	72.7	13.0	7	< 0.05 for size; > 0.05 for seamount
<i>Diaphus suborbitalis</i>	$\delta^{15}\text{N} = 11.5 - 0.0151 \times \text{SL} + 0.7594 \times \text{seamount}$	43.8	4.51	7	> 0.05 for size; < 0.05 for seamount
<i>Abraliopsis</i> sp.	$\delta^{15}\text{N} = 10.3 + 0.0069 \times \text{DML} - 1.006 \times \text{seamount}$	56.2	8.06	9	> 0.05 for size; < 0.05 for seamount
<i>Chauliodus sloani</i>	$\delta^{15}\text{N} = 10.2 - 0.0065 \times \text{SL} + 0.7431 \times \text{seamount}$	12.5	1.64	7	> 0.05 for size and seamount
Leptocephali larvae	$\delta^{15}\text{N} = 7.18 - 0.0170 \times \text{TL} - 1.1971 \times \text{seamount}$	25.3	2.69	8	> 0.05 for size and seamount